Accepted Manuscript

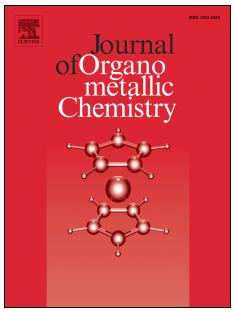

Reversible C-H bond activation at a triosmium centre: A comparative study of the reactivity of unsaturated triosmium clusters $Os_3(CO)_8(\mu\text{-dppm})(\mu\text{-H})_2$ and $Os_3(CO)_8(\mu\text{-dppf})(\mu\text{-H})_2$ with activated alkynes

Md. Arshad H. Chowdhury, Mohd. Rezaul Haque, Shishir Ghosh, Shaikh M. Mobin, Derek A. Tocher, Graeme Hogarth, Michael G. Richmond, Shariff E. Kabir, Herbert W. Roesky

PII: S0022-328X(17)30132-8

DOI: 10.1016/j.jorganchem.2017.02.041

Reference: JOM 19830

To appear in: *Journal of Organometallic Chemistry*

Received Date: 3 December 2016

Revised Date: 24 February 2017

Accepted Date: 25 February 2017

Please cite this article as: M.A.H. Chowdhury, M.R. Haque, S. Ghosh, S.M. Mobin, D.A. Tocher, G. Hogarth, M.G. Richmond, S.E. Kabir, H.W. Roesky, Reversible C-H bond activation at a triosmium centre: A comparative study of the reactivity of unsaturated triosmium clusters $Os_3(CO)_8(\mu\text{-dppm})(\mu\text{-H})_2$ and $Os_3(CO)_8(\mu\text{-dppf})(\mu\text{-H})_2$ with activated alkynes, *Journal of Organometallic Chemistry* (2017), doi: 10.1016/j.jorganchem.2017.02.041.

Graphical Abstract

Reversible C-H bond activation at a triosmium centre: A comparative study of the reactivity of unsaturated triosmium clusters $Os_3(CO)_8(\mu\text{-dppm})(\mu\text{-H})_2$ and $Os_3(CO)_8(\mu\text{-dppf})(\mu\text{-H})_2$ with activated alkynes

Md. Arshad H. Chowdhury, Mohd. Rezaul Haque, Shishir Ghosh, Shaikh M. Mobin, Derek A. Tocher, Graeme Hogarth, Michael G. Richmond, Shariff E. Kabir, Herbert W. Roesky

The reactivity of two unsaturated triosmium clusters $Os_3(CO)_8(\mu\text{-dppm})(\mu\text{-H})_2$ and $Os_3(CO)_8(\mu\text{-dppf})(\mu\text{-H})_2$ toward activated alkynes has been investigated.

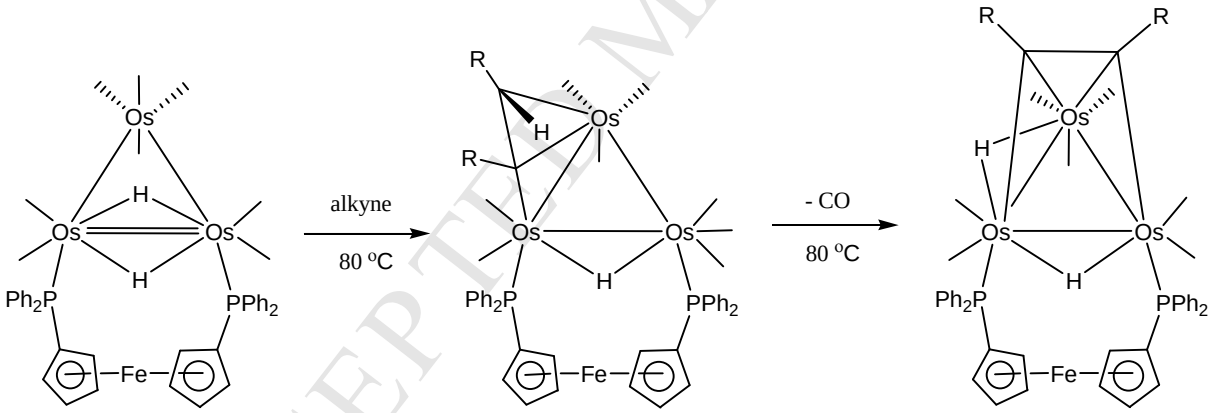

alkenyl

alkyne and hydride

Reversible C-H bond activation at a triosmium centre: A comparative study of the reactivity of unsaturated triosmium clusters $Os_3(CO)_8(\mu\text{-dppm})(\mu\text{-H})_2$ and $Os_3(CO)_8(\mu\text{-dppf})(\mu\text{-H})_2$ with activated alkynes

Md. Arshad H. Chowdhury [a], Mohd. Rezaul Haque [a], Shishir Ghosh [a], Shaikh M. Mobin [b], Derek A. Tocher [c], Graeme Hogarth [d], Michael G. Richmond [e], Shariff E. Kabir [a,f,*], Herbert W. Roesky [f,*]

[a] *Department of Chemistry, Jahangirnagar University, Savar, Dhaka 1342, Bangladesh*

[b] *Discipline of Chemistry, School of Basic Science, Indian Institute of Technology Indore, Khandwa Road, Indore 452 017, India*

[c] *Department of Chemistry, University College London, 20 Gordon Street, London, WC1H 0AJ, United Kingdom.*

[d] *Department of Chemistry, King's College London, Britannia House, 7 Trinity Street, London SE1 1DB, UK*

[e] *Department of Chemistry, University of North Texas, Denton, Texas 76203, USA*

[f] *Georg-August University, Institute of Inorganic Chemistry, Tammannstr. 4, D-37077 Göttingen, Germany*

*Corresponding authors. E-mail address: skabir_ju@yahoo.com (S. E. Kabir), hroesky@gwdg.de (H. W. Roesky)

ABSTRACT

Heating a benzene solution of the unsaturated cluster $Os_3(CO)_8(\mu\text{-dppm})(\mu\text{-H})_2$ (**1**) [dppm = bis(diphenylphosphino)methane] with $MeO_2CC{\equiv}CCO_2Me$ (DMAD) or $EtO_2CC{\equiv}CCO_2Et$ (DEAD) at 80 °C furnished the dinuclear compounds $Os_2(CO)_4(\mu\text{-dppm})(\mu\text{-}\eta^2;\eta^1;\kappa^1\text{-}RO_2CCCHCO_2R)(\mu\text{-H})$ (**3a**, R = Me, **3b**, R = Et) and the saturated trinuclear complexes $Os_3(CO)_7(\mu\text{-dppm})(\mu_3\text{-}\eta^2;\eta^1;\eta^1\text{-}RO_2CCCCO_2R)(\mu\text{-H})_2$ (**4a**, R = Me, **4b**, R = Et). In contrast, similar reactions using unsaturated $Os_3(CO)_8(\mu\text{-dppf})(\mu\text{-H})_2$ (**2**) [dppf =

bis(diphenylphosphino)ferrocene] afforded only the trinuclear complexes $Os_3(CO)_8(\mu\text{-dppf})(\mu\text{-}\eta^2;\eta^1\text{-}RO_2CCHCCO_2R)(\mu\text{-H})$ (**5a**, R = Me; **5b**, R = Et) and $Os_3(CO)_7(\mu\text{-dppf})(\mu_3\text{-}\eta^2;\eta^1;\eta^1\text{-}RO_2CCCCO_2R)(\mu\text{-H})_2$ (**6a**, R = Me; **6b**, R = Et). Control experiments confirm that **5a** and **5b** decarbonylate at 80 °C to give **6a** and **6b**, respectively. Both **5a** and **5b** exist as a pair of isomers in solution, as demonstrated by ^{1}H NMR and $^{31}P\{^1H\}$ NMR spectroscopy. DFT calculations on cluster **5a** (as the dppf-Me_4 derivative) indicate that the isomeric mixture derives from a torsional motion that promotes the conformational flipping of the cyclopentadienyl groups of the dppf-Me_4 ligand relative to the metallic plane. VT NMR measurements on clusters **6a** and **6b** indicate that while the hydride ligand associated with the dppf-bridged Os-Os bond is nonfluxional at room temperature, the second hydride rapidly oscillates between the two non-dppf-bridged Os-Os edges. DFT examination of this hydride fluxionality confirms a "windshield wiper" motion for the labile hydride that gives rise to a time-average coupling of this hydride to both phosphorus centers of the dppf ligand. Thermolysis of **6a** and **6b** in refluxing toluene yielded $Os_3(CO)_7(\mu\text{-dppf})(\mu\text{-}\eta^2;\eta^1;\kappa^1\text{-}CCHCO_2R)$ (**7a**, R= Me; **7b**, R= Et). The vinylidene moieties in **7a** and **7b** derive from the carbon-carbon bond cleavage of coordinated alkyne ligands, and these two products exhibit high thermal stability in refluxing toluene.

Keywords: Unsaturated osmium clusters; Diphosphines; Reversible C-H bond activation; Aactivated alkynes; C-C bond scission; DFT.

1. Introduction

Over the past three decades, the chemistry of triosmium complexes bearing a bridging bis(diphenylphosphino)methane (dppm) ligand has received considerable attention because of their interesting chemistry, giving rise to many novel and potentially useful compounds [1-12]. In contrast, fewer examples of triosmium carbonyl cluster complexes containing the more flexible backbone functionalized derivative, 1,1'-bis(diphenylphosphino)ferrocene (dppf), have been reported [12-14]. The high reactivity associated with electronic and coordinative unsaturation in mononuclear transition metal complexes has been extensively studied due to their potential catalytic applications and interesting chemistry [15]. In comparison and notwithstanding the widespread interest in cluster chemistry, the number of unsaturated clusters is limited [1, 15-17]. Among these, the most studied example of electronically unsaturated

cluster is $Os_3(CO)_{10}(\mu\text{-}H)_2$ [17, 18] which is unsaturated based on its 46e count, and it exhibits rich and diverse chemistry that includes fundamental bond activation processes at a wide range of substrates. The reactivity of this unsaturated cluster towards alkynes was studied with particular interest since coordinatively unsaturated hydride complexes play an important role in various homogeneous catalytic processes [19].

The coordination of an alkyne to trinuclear metal complexes depends on both the metal and the substituents on the alkyne [20]. Such reactions lead to a number of different products, with hydrometalation to yield alkenyl complexes being the most prevalent. As early as 1984, Mays and Dawoodi [18i] demonstrated that $Os_3(CO)_{10}(\mu\text{-}H)_2$ reacts with the activated alkyne $CF_3C{\equiv}CCF_3$ to give the zwitterionic alkenyl complex $Os_3CO)_{10}[\mu_3\text{-}CF_3CCC(H)CF_3](\mu\text{-}H)$ in which the hydrocarbyl fragment caps the osmium triangle. Smith and coworkers reported that the reaction of the orthometalated dppm derivative $Os_3(CO)_8[\mu\text{-}Ph_2PCH_2P(Ph)C_6H_4](\mu\text{-}H)$, another example of an interesting 46-electron triosmium hydride cluster, with diphenylacetylene led to the formation of the 46e cluster $Os_3(CO)_7(PhC{\equiv}CPh)(\mu\text{-dppm})$, in which the alkyne was bonded in a $\mu_3\text{-}\eta^2(\perp)$ mode. They also reported that the addition of CO to the latter resulted in $Os_3(CO)_7(\mu\text{-CO})(PhC{\equiv}CPh)(\mu\text{-dppm})$ in which the alkyne is bonded in a $\mu_3\text{-}\eta^2(\parallel)$ mode [3a,b]. Recently, we also reported the reactions of $Os_3(CO)_9(\mu_3\text{-benzoheterocycle})(\mu\text{-}H)$, another type of electronically unsaturated triosmium cluster, with alkynes which yielded various products via insertion of alkynes into the metal-hydride bond [21].

Although the reactivity of the unsaturated cluster $Os_3(CO)_{10}(\mu\text{-}H)_2$ has extensively been investigated [17, 18], few studies have hitherto been published involving the dppm and dppf derivatives $Os_3(CO)_8(\mu\text{-dppm})(\mu\text{-}H)_2$ (**1**) and $Os_3(CO)_8(\mu\text{-dppf})(\mu\text{-}H)_2$ (**2**). In a recent contribution, we reported the reactivity of the unsaturated compounds **1** and **2** towards Ph_3SnH, which is highly dependent on the nature of diphosphines [12]. With the rigid dppm ligand in **1**, the stannylene complex $Os_3(CO)_7(\mu\text{-}SnPh_2)_2(\mu\text{-dppm})(H)_2$ was the major product, resulting from both Sn-H and Sn-C bond activation in addition to the minor products $Os_3(CO)_8(SnPh_3)_2(\mu\text{-dppm})(\mu\text{-}H)_2$ and $Os_3(CO)_8(SnPh_3)\{\mu\text{-}Ph_2PCH_2P(Ph)C_6H_4\}(\mu\text{-}H)_2$. Cluster **2** containing the highly flexible dppf ligand gives a mixture of mono-, di- and triosmium complexes that include

$Os(CO)_4(SnPh_3)H$, $Os_2(CO)_4(SnPh_3)_2(\mu\text{-}HSnPh_2)(\mu\text{-}dppf)(\mu\text{-}H)$ and $Os_3(CO)_8(SnPh_3)(\mu\text{-}dppf)H(\mu\text{-}H)_2$ [12].

Exposing the previously reported reactivity of electron-deficient triosmium clusters toward alkynes and the reactivity of the resulting alkyne derivatives, we thought it would be useful to perform a similar study of the reactions of activated alkynes with unsaturated triosmium hydride clusters $Os_3(CO)_8(\mu\text{-}dppm)(\mu\text{-}H)_2$ (**1**) and $Os_3(CO)_8(\mu\text{-}dppf)(\mu\text{-}H)_2$ (**2**). These show significant difference in reactivity depending on the flexibility of diphosphine. Herein we report our results on the reactions of the activated alkynes DMAD and DEAD with **1** and **2** which are quite different as expected. New modes of cluster reactivity are demonstrated, and the resulting products characterized by a combination of spectroscopic methods and X-ray diffraction analyses.

2. Experimental Section

2.1. General procedures

Unless otherwise stated, all reactions were carried out under a dry nitrogen atmosphere using standard Schlenk techniques. Reagent-grade solvents were dried using appropriate drying agents and distilled prior to use by standard methods. Infrared spectra were recorded on a Shimadzu FTIR 8101 spectrophotometer, and NMR spectra were recorded on a Varian Unity Plus 500 spectrometer. All chemical shifts are reported in δ units and are referenced to the residual protons of the deuterated solvents (^1H) and to external H_3PO_4 (^{31}P). Elemental analyses were performed by the Microanalytical Laboratories of the Wazed Miah Science Research Center at Jahangirnagar University. DMAD and DEAD were purchased from Aldrich Chemical Co. and used without further purification. Clusters $Os_3(CO)_8(\mu\text{-}dppm)(\mu\text{-}H)_2$ [22] and $Os_3(CO)_8(\mu\text{-}dppf)(\mu\text{-}H)_2$ [13] were prepared according to the literature procedures. Product separations were performed by TLC in air on 0.5 mm silica gel (GF_{254}-type 60, E. Merck, Germany) glass plates.

*2.2. Reaction of $Os_3(CO)_8(\mu\text{-dppm})(\mu\text{-H})_2$(**1**) with DMAD at 80 °C*

A benzene solution (20 mL) of **1** (50 mg, 0.042 mmol) and DMAD (30 mg, 0.21 mmol) was heated to reflux for 4 h. The solvent was removed under reduced pressure and the residue separated by TLC on silica gel. Elution with cyclohexane/CH_2Cl_2 (3:2, v/v) developed four bands. The first band was unreacted **1** (trace) and the second band afforded $Os_2(CO)_4(\mu\text{-dppm})(\mu\text{-}\eta^2;\eta^1;\kappa^1\text{-}MeO_2CCCHCO_2Me)(\mu\text{-H})$ (**3a**) (18 mg, 24%) as pale yellow crystals, while the third band gave $Os_3(CO)_7(\mu\text{-dppm})(\mu_3\text{-}\eta^2;\eta^1;\eta^1\text{-DMAD})(\mu\text{-H})_2$ (**4a**) (15 mg, 27%) as red crystals after recrystallization from hexane/CH_2Cl_2 at 4 °C. The fourth band was too small for complete characterization. Spectral data for **3a**: Anal. Calcd for $C_{35}H_{30}O_8Os_2P_2\cdot 2CH_2Cl_2$: C, 37.32; H, 2.88. Found: C, 37.63; H, 2.95. IR (νCO, CH_2Cl_2): 2031 s, 1997 vs, 1963 vs,1925 s cm^{-1}. ^1H NMR ($CDCl_3$): δ 7.68 (m, 2H), 7.54 (m, 2H), 7.48 (m, 1H), 7.39 (m, 2H), 7.26 (m, 3H), 7.18 (m, 3H), 7.07 (m, 2H), 7.01 (m, 3H), 6.86 (m, 2H), 5.32 (s, CH_2Cl_2), 4.75 (d, J 24, 15 Hz, 1H), 4.43 (d, J 5 Hz, 1H), 4.01 (d, J 24, 15 Hz, 1H), 3.77 (s, 3H), 3.66 (s, 3H), -12.92 (dd, J 9, 7 Hz, 1H). $^{31}P\{^1H\}$ NMR($CDCl_3$): δ -2.3 (d, J 52 Hz, 1P), -11.9 (d, J 52 Hz, 1P). Spectral data for **4a**: Anal. Calcd for $C_{38}H_{30}O_{11}Os_3P_2$: C, 35.24; H, 2.34. Found: C, 35.41; H, 2.53. IR (νCO, CH_2Cl_2): 2070 vs, 2035 s, 2013 s, 1990 vs cm^{-1}. ^1H NMR ($CDCl_3$): δ 7.58 (m, 2H), 7.49 (m, 2H), 7.43 (m, 1H), 7.35 (m, 2H), 7.21 (m, 3H), 7.13 (m, 3H), 7.02 (m, 2H), 6.96 (m, 3H), 6.81 (m, 2H), 4.71 (m, 1H), 3.97 (m, 1H), 3.73 (s, 3H), 3.63 (s, 3H), -15.90 (t, J 11.5 Hz, 1H), -19.85 (d, J 33 Hz, 1H). $^{31}P\{^1H\}$ NMR($CDCl_3$): δ -21.5 (d, J 45 Hz, 1P), -23.4 (d, J 45 Hz, 1P).

*2.3. Reaction of **1** with DEAD at 80 °C*

The reaction of **1** (50 mg, 0.042 mmol) and DEAD (36 mg, 0.21 mmol) followed a protocol similar to that described in the above procedure. Here the workup afforded $Os_2(CO)_4(\mu\text{-dppm})(\mu\text{-}\eta^2;\eta^1;\kappa^1\text{-}EtO_2CCCHCO_2Et)(\mu\text{-H})$ (**3b**) (13 mg, 29%) as pale yellow crystals and $Os_3(CO)_7(\mu\text{-dppm})(\mu_3\text{-}\eta^2;\eta^1;\eta^1\text{-DEAD})(\mu\text{-H})_2$ (**4b**) (9 mg, 16%) as red crystals from hexane/CH_2Cl_2 at 4 °C. Spectral data for **3b**: Anal. Calcd. for $C_{37}H_{34}O_8Os_2P_2$: C, 42.36; H, 3.27. Found: C, 42.50; H, 3.41%. IR (νCO, CH_2Cl_2): 2031 s, 1996 vs, 1962 vs, 1924 s cm^{-1}. ^1H NMR ($CDCl_3$): δ 7.68 (m, 2H), 7.54 (m, 2H), 7.47(m, 1H), 7.40 (m, 2H), 7.26 (m, 3H), 7.17(m, 3H),

7.03 (m, 5H), 6.86 (m, 2H), 4.82 (m, 1H), 4.47 (d, J 8 Hz, 1H), 4.35 (m, 1H), 4.08 (m, 4H), 1.29 (t, J 6 Hz, 3H), 1.23 (t, J 8 Hz, 3H), -12.93 (dd, J 12, 8 Hz). $^{31}P\{^{1}H\}$ NMR($CDCl_3$): δ -2.1 (d, J 52 Hz, 1P), -11.8 (d, J 52 Hz, 1P). Spectral data for **4b**: Anal. Calcd. for $C_{40}H_{34}O_{11}Os_3P_2$: C, 36.31; H, 2.59. Found: C, 36.82; H, 2.65. IR (νCO, CH_2Cl_2): 2069 vs, 2035 s, 2012 s, 1989 s cm^{-1}. ^{1}H NMR ($CDCl_3$): δ 7.56 (m, 5H), 7.38 (m, 6H), 7.22 (m, 9H), 4.41 (m, 2H), 4.25 (m, 1H), 4.13 (m, 1H), 3.94 (m, 2H), 1.31 (t, J 7.5 Hz, 3H), 1.0 (t, J 7.5 Hz, 3H), -15.77 (dd, J 16, 12 Hz, 1H), -19.81 (d, J 32 Hz, 1H). $^{31}P\{^{1}H\}$ NMR ($CDCl_3$): δ -22.1 (d, J 44 Hz, 1P), -23.7 (d, J 44 Hz, 1P).

*2.4. Reaction of **1** with DMAD at 110 °C*

A toluene solution (20 mL) of **1** (50 mg, 0.042 mmol) and DMAD (30 mg, 0.21 mmol) was heated to reflux for 3 h. A similar chromatographic separation and work up described above afforded only **3a** (26 mg, 35%).

*2.5. Reaction of **1** with DEAD at 110 °C*

A mixture of **1** (50 mg, 0.042 mmol) and DEAD (36 mg, 0.21 mmol) was heated in boiling toluene (20 mL) for 3h. A similar chromatographic separation and work up described above furnished only **3b** (19 mg, 42%).

*2.6. Thermolysis of **4a** and **4b***

A toluene solution (15 mL) of **4a** (15 mg, 0.012 mmol) was heated for 2 h maintaining the bath temperature 80 °C. The reaction mixture did not show any significant change during this period. The bath temperature was then raised to 110 °C and heating was continued for further 2 h which led to unspecific decomposition. A similar chromatographic separation described above led to the recovery of unreacted **4a** (7 mg) only. Thermal treatment of **4b** following the abovementioned protocol showed similar results i.e., only led to the recovery of unreacted **4b** (5 mg).

*2.7. Reaction of $Os_3(CO)_8(\mu\text{-dppf})(\mu\text{-H})_2$ (**2**) with DMAD*

A benzene solution (30 mL) of **2** (0.10 g, 0.075 mmol) and DMAD (45 µL, 0.37 mmol) was heated to reflux for 2.5 h, during which time the color of the solution changed from green to yellow. The solvent was removed under reduced pressure and the residue chromatographed by TLC on silica gel. Elution with cyclohexane/CH_2Cl_2 (1:1, v/v) developed two bands which afforded, in order of elution, $Os_3(CO)_8(\mu\text{-dppf})(\mu_3\text{-}\eta^2;\eta^1\text{-}MeO_2CCHCCO_2Me)(\mu\text{-H})$ (**5a**) (17 mg, 30%) and $Os_3(CO)_7(\mu\text{-dppf})(\mu_3\text{-}\eta^2;\eta^1;\eta^1\text{-DMAD})(\mu\text{-H})_2$ (**6a**) (25 mg, 46%) as yellow crystals after recrystallization from hexane/CH_2Cl_2 at -4 °C. Spectral data for **5a**: Anal. Calcd. for $C_{48}H_{36}FeO_{12}Os_3P_2\cdot CH_2Cl_2$: C, 37.29; H, 2.43. Found: C, 37.65; H, 2.54.IR (νCO, CH_2Cl_2): 2077 s, 2037 vs, 2013 vs, 1990 vs, 1966 w cm^{-1}. ^1H NMR ($CDCl_3$): both isomer, δ 7.74 (m, 6H), 7.61-7.56 (m, 12H), 7.46 (m, 3H), 7.37 (m, 8H), 7.29 (m, 3H), 7.14 (m, 2H), 7.07 (m, 6H), 5.30 (s, CH_2Cl_2), 5.01 (s, 1H), 4.83 (s, 1H), 4.38 (s, 1H), 4.35 (s, 1H), 4.30 (s, 1H), 4.26 (s, 2H), 4.13 (s, 1H), 3.97 (s, 1H), 3.85 (s, 1H), 3.77 (s, 2H), 3.70 (s, 1H), 3.67 (s, 3H), 3.64 (s, 3H), 3.60 (s, 1H), 3.56 (s, 2H), 3.41 (s, 3H), 2.98 (s, 3H), -17.67 (t, J 10 Hz, 1H), -17.81 (dd, J 15, 10 Hz). $^{31}P\{^1H\}$ NMR ($CDCl_3$): both isomer, δ 3.1 (s, 1P), -6.0 (s, 1P), -8.3 (s, 1P), -9.0 (s, 1P). Spectral data for **6a**: Anal. Calcd. for $C_{47}H_{36}FeO_{11}Os_3P_2$: C, 38.53; H, 2.48. Found: C, 38.75; H, 2.66. IR (νCO, CH_2Cl_2): 2076 vs, 2035 s, 2011 s, 1970 w, 1941 w cm^{-1}. ^1H NMR (25 °C, $CDCl_3$): δ 7.53 (m, 4H), 7.42 (m, 16H), 4.34 (s, 2H), 4.18 (s, 2H), 4.07 (s, 2H), 3.98 (m, 2H), 3.41 (s, 6H), -16.65 (t, J 10 Hz, 1H), -19.80 (t, J 10 Hz, 1H). $^{31}P\{^1H\}$ NMR ($CDCl_3$, -40 ^oC): δ 3.2 (s, 1P), -9.7 (s, 1P).

*2.8. Reaction of **2** with DEAD*

A solution of **2** (0.10 g, 0.075 mmol) and DEAD (59 µL, 0.37 mmol) in benzene (30 mL) was heated to reflux for 3 h. The solvent was removed under reduced pressure and the residue chromatographed by TLC on silica gel. Elution with cyclohexane/CH_2Cl_2 (1:1, v/v) afforded two bands, which gave the following compounds in order of elution, $Os_3(CO)_8(\mu\text{-dppf})(\mu\text{-}\eta^2;\eta^1\text{-}EtO_2CCHCCO_2Et)(\mu\text{-H})$ (**5b**) (15 mg, 26%) and $Os_3(CO)_7(\mu\text{-dppf})(\mu_3\text{-}\eta^2;\eta^1;\eta^1\text{-DEAD})(\mu\text{-H})_2$ (**6b**) (24 mg, 63%) as yellow crystals after recrystallization from hexane/CH_2Cl_2 at -4 °C.

Spectral data for **5b**: Anal. Calcd for $C_{50}H_{40}FeO_{12}Os_3P_2$: C 39.46; H 2.65. Found: C 39.62; H, 2.78%. IR (νCO, CH_2Cl_2): 2077 vs, 2036 vs, 2012 vs, 1990s, 1967w cm^{-1}. ^1H NMR ($CDCl_3$): both isomer (aromatic protons), δ 7.76 (m, 5H), 7.60 (m, 5H), 7.55 (m, 6H), 7.46-7.37 (m, 16H), 7.29 (m, 2H), 7.14 (m, 1H), 7.07 (m, 5H); major isomer (Cp and Et protons), 4.30 (s, 1H), 4.25 (s, 1H), 4.14 (m, 3H), 3.96 (s, 1H), 3.91 (m, 4H), 3.90 (s, 1H), 3.78 (s, 1H), 3.70 (s, 1H), 1.24 (t, 10 Hz, 3H), 0.85 (t, 10Hz, 3H), minor isomer (Cp and Et protons), 4.83 (s, 1H), 4.34 (s, 1H), 4.27 (s, 1H), 3.94 (s, 1H), 3.87 (s, 1H), 3.82 (m, 2H), 3.75 (s, 1H), 3.61 (s, 1H), 3.51 (s, 1H), 3.46 (m, 2H), 1.00 (t, 10 Hz, 3H), 0.72 (t, 10 Hz, 3H); major isomer (hydride), -17.69 (t, J 10 Hz, 1H), minor isomer (hydride), -17.76 (t, J 10 Hz, 1H). $^{31}P\{^1H\}$ NMR ($CDCl_3$): major isomer, δ 3.0 (s, 1P), -8.4 (s, 1P); minor isomer, δ -6.0 (s, 1P), -8.9 (s, 1P). Spectral data for **6b**: Anal. Calcd. for $C_{49}H_{40}FeO_{11}Os_3P_2$: C, 39.41; H, 2.70. Found: C, 39.61; H, 2.85%. IR (νCO, CH_2Cl_2): 2076 vs, 2035 vs, 2010 vs, 1970 m, 1941m cm^{-1}. ^1H NMR ($CDCl_3$): δ 7.56 (br, m, 4H), 7.42 (m, 16H), 4.08 (br, 2H), 3.94 (overlapping singlets, 6H), 3.83 (m, 4H), 1.00 (t, J 10 Hz, 6H), -16.70 (t, J 10 Hz, 1H), -19.12 (t, J 10 Hz, 1H). $^{31}P\{^1H\}$ NMR ($CDCl_3$, 25 °C): δ -6.5(br, s).

*2.9. Conversion of **5a** to **6a***

A benzene solution (20 mL) of **5a** (20 mg, 0.075 mmol) was heated to reflux for 3 h. The solvent was removed under reduced pressure and the residue was chromatographed by TLC on silica gel. Elution with cyclohexane/CH_2Cl_2 (1:1, v/v) developed two bands. The major band afforded **6a** (18 mg, 89%), while the minor band gave unreacted **5a** (trace).

*2.10. Conversion of **5b** to **6b***

A similar thermolysis of **5b** (20 mg, 0.075 mmol), following the above mentioned protocol, at 80 °C for 3.5 h afforded **6b** (18 mg, 90%) after chromatographic separation and workup.

*2.11. Thermolysis of **6a***

A toluene solution (20 mL) of **6a** (25 mg, 0.017 mmol) was heated to reflux for 3.5 h. The solvent was removed under reduced pressure and the residue chromatographed by TLC on silica gel. Elution with cyclohexane/CH_2Cl_2 (1:1, v/v) developed two bands. The major band gave $Os_3(CO)_7(\mu\text{-dppf})(\mu\text{-}\eta^2;\eta^1;\kappa^1\text{-}CCHCO_2CH_3)$ (**7a**) (24 mg, 50%) as yellow crystals after recrystallization from hexane/CH_2Cl_2 at -4 °C, and the minor band (trace) was not characterized. Spectral data for **7a**: Anal. Calcd for $C_{45}H_{32}FeO_9Os_3P_2$: C, 38.46; H, 2.30. Found: C, 38.65; H, 2.48. IR (νCO, CH_2Cl_2): 2038 vs, 1989 s, 1959 w, 1942 sh cm^{-1}. ^1H NMR ($CDCl_3$): δ 8.07 (m, 2H), 7.76 (m, 3H), 7.58 (m, 4H), 7.51 (m, 4H), 7.32 (m, 3H), 7.20 (m, 4H), 7.01 (m, 1H), 5.33 (s, 1H), 5.04 (s, 1H), 4.32 (s, 1H), 4.25 (s, 1H), 4.09 (s, 1H), 3.81 (s, 1H), 3.73 (s, 1H), 3.70 (s, 1H), 3.33 (s, 1H), 2.83 (s, 3H). $^{31}P\{^1H\}$ NMR ($CDCl_3$): δ 14.5 (s, 1P), 7.1 (s, 1P).

*2.12. Thermolysis of **6b***

A similar thermolysis of **6b** (25 mg, 0.016 mmol) at 110 °C for 3.5 h gave $Os_3(CO)_7(\mu\text{-dppf})(\mu\text{-}\eta^2;\eta^1;\kappa^1\text{-}CCHCO_2Et)$ (**7b**) (12 mg, 48%) as yellow crystals after recrystallization from hexane/CH_2Cl_2 at -4 °C. Spectral data for **7b**: Anal. Calcd. for $C_{46}H_{34}FeO_9Os_3P_2\cdot CH_2Cl_2$: C, 37.53; H, 2.41. Found: C, 37.76; H, 2.65. IR (νCO, CH_2Cl_2): 2038 vs, 1989 s, 1959 m, 1943 sh cm^{-1}. ^1H NMR ($CDCl_3$): δ 8.07 (m, 2H), 7.74 (m, 3H), 7.58 (m, 4H), 7.48 (m, 5H), 7.32 (m, 1H), 7.19 (m, 3H), 7.01 (m, 2H), 5.33 (s, 1H), 5.30 (s, CH_2Cl_2), 5.28 (s, 1H), 5.04 (s, 1H), 4.32 (s, 1H), 4.24 (s, 1H), 4.10 (s, 1H), 3.81 (s, 1H), 3.70 (s, 1H), 3.34 (s, 1H), 3.19 (m, 1H), 2.93 (m, 1H), 0.96 (t, J 10 Hz, 3H). $^{31}P\{^1H\}$ NMR ($CDCl_3$): δ 14.2 (s, 1P), 6.8 (s, 1P).

2.13. X-ray crystallography

Single crystals of **3a, 4b, 5a, 6a, 6b**, and **7b** suitable for single-crystal X-ray diffraction analyses were mounted on Nylon loops with inert oil or Apiezon grease. For compound **3a**, data were collected on a Bruker D8 SMART APEX CCD diffractometer. For compound **4b**, data were collected on a Rigaku XtaLab mini bench-top diffractometer. Data for compounds **5a**, **6a**, **6b** and **7b** were measured on an Agilent Technologies Super Nova diffractometer. Data collection temperatures and X-ray sources are reported in Table 1 together with other crystallographic

details. Data reduction and absorption corrections were carried out using SAINT+ and SADABS [23] for **3a** and with Crystal Clear [24] for **4b**. For compounds **5a**, **6a**, **6b** and **7b**, data reduction and absorption corrections were carried out with Crysalis Pro [25]. Structures were solved by direct methods and refined by difference fourier synthesis using the SHELX [26] suite of programs within either the WinGX [27] or Olex 2 [28] graphical user interfaces. Non-hydrogen atoms were refined anisotropically and hydrogens included using a riding model. Hydride ligands were located as weak features in the final electron density maps. The quality of the single crystals of **5a** available for XRD analysis was relatively poor which led to the collection of low quality data hence the resolution of the data set for this complex is poor.

2.14. Computational Methodology

The DFT calculations were carried out with the Gaussian 09 package of programs [29] using the B3LYP hybrid functional. This functional is comprised of Becke's three-parameter hybrid exchange functional (B3) [30] and the correlation functional of Lee, Yang, and Parr (LYP) [31]. The iron and osmium atoms were described with the Stuttgart-Dresden effective core potential and SDD basis set [32], and the 6-31G(d') basis set [33] was employed for the P, O, C, and H atoms. To facilitate the calculations, the phenyl groups on the dppf ligand were replaced with methyl groups (dppf-Me_4).

The reported geometries for clusters **A-D_alt** were fully optimized, and the analytical Hessian was evaluated at each stationary point to confirm that the geometry was an energy minimum (no negative eigenvalues). Intrinsic reaction coordinate (IRC) calculations were performed on **TSDD_alt** in order to establish the reactant and product species associated with this transition-state structure. Unscaled vibrational frequencies were used to make zero-point and thermal corrections to the electronicenergies and the resulting free energies are reported in kcal/mol relative to the specified standard. Standard state corrections were applied to all species to convert concentrations from 1 atm to 1 M according to the treatise of Cramer [34]. The geometry-optimized structures have been drawn with the *JIMP*2 molecular visualization and manipulation program [35].

3. Results and discussion

*3.1. Reactions of $Os_3(CO)_8(\mu\text{-dppm})(\mu\text{-H})_2$ (**1**) with DMAD and DEAD*

Refluxing cluster **1** with DMAD or DEAD in benzene afforded the dinuclear compounds $Os_2(CO)_4(\mu\text{-dppm})(\mu\text{-}\eta^2;\eta^1;\kappa^1\text{-}RO_2CCCHCO_2R)(\mu\text{-H})$ (**3a,** R = Me, 24%; **3b,** R = Et, 29%) and the saturated trinuclear complexes $Os_3(CO)_7(\mu\text{-dppm})(\mu_3\text{-}\eta^2;\eta^1\text{-}RO_2CCCCO_2R)(\mu\text{-H})_2$ (**4a,** R = Me, 27%; **4b,** R = Et, 16%) after chromatographic separation. Scheme 1 highlights the results of the reaction of cluster **1** with the two alkynes. The formation of dinuclear products in this reaction is consistent with that observed from the photochemical reaction of $Os_3(CO)_{12}$ with DMAD [36]. Compounds **3a** and **3b** were the only products isolated when the same reactions were carried out in toluene at 110 °C. Heating compounds **4a** and **4b** at 80-110 °C did not produce any of **3a** and **3b** indicating that these trinuclear clusters do not serve as precursor for the dinuclear products i.e., they are formed via different reaction pathways. Both the dinuclear compounds were characterized by a combination of elemental analyses, infrared and ^1H and $^{31}P\{^1H\}$ NMR spectroscopy, together with a single crystal X-ray diffraction analysis for **3a**.

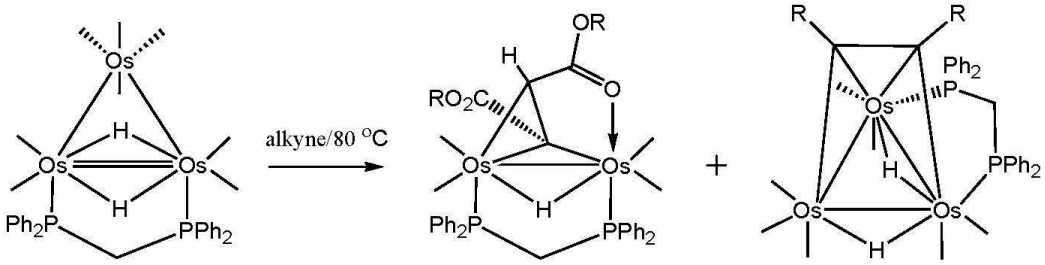

Scheme 1

An ORTEP diagram of the molecular structure of **3a** is depicted in Fig. 1 and selected bond distances and angles are quoted in the caption. The molecule has 34 valence electrons and consists of a dinuclear framework of two osmium atoms where the Os-Os bond is spanned by

edge-bridging hydride and dppm ligands. Each osmium center contains two terminal CO groups and bonded to "flyover" μ-η^2;η^1;κ^1-$MeO_2CCCHCO_2Me$ ligandwhich functions as a 5e donor. It is coordinated to the dimetallic centre through the alkenyl functionality in a σ,π-vinyl fashion in such a way that the C(5) carbon is coordinated to Os(1) through an Os-C σ-bond [Os(1)-C(5) 2.143(8) Å)] and a π interaction between C(5)-C(6) and Os(2) [Os(2)C(5) 2.141(8) Å and Os(2)-C(6) 2.177(9) Å]. The alkenyl carbon, C(6), is also bonded to a hydrogen atom. A similar bonding mode of the alkenyl ligand was reported in the diiron compound $Fe_2(CO)_4(\mu$-$PPh_2)(\mu$-dppm)(μ-η^2;η^1-$MeO_2CCCHCO_2Me$), obtained from the reaction of $Fe_2(CO)_4(\mu$-H)(μ-CO)(μ-$PPh_2)(\mu$-dppm) with DMAD [37]. There is also an additional bonding interaction between a carbonyl oxygen, O(5), of one of the carboxylate groups and the Os(1) atom. The C(5)-C(6) bond distance in **3a** [1.460(11)] is significantly shorter than the expected sp^3-sp^3 carbon-carbon single bond distance and is very similar to the carbon-carbon bond distance in $Os_3(CO)_9(\mu$-η^2;η^1;κ^1-$MeO_2CCCHCO_2Me)(\mu$-$C_7H_4NS)$ [21a]. The conversion of the alkyne to an alkenyl moiety is facilitated by the transfer of one of the original hydride ligands in **1** to the DMAD substrate. The Os-Os distance of 2.9254(6) Å in **3a** is slightly longer that found in $Os_2(CO)_8(\mu$-η^1;η^1-DMAD) [36] [2.8975(1)Å] and $Os_2(CO)_8(\mu$-η^1;η^1-$CH_2CHCO_2Me)$ [38] (2.8850(1) Å). The Os-P bond lengths in **3a**, while are asymmetrical in nature, [Os(1)-P(1) 2.303(2), Os(2)-P(2) 2.346(2) Å] agree with those Os-P bond distances reported for the parent compound **1** [1b] [2.336(5) and 2.337(5) Å] whose Os-P bond distances that are highly symmetrical.

Place Figure One Here

The spectroscopic data for **3a** are consistent with the solid-state structure. Moreover, the spectral data for **3b** closely parallel the data recorded for **3a**, confirming that both products possess a similar structure. The IR spectra recorded for **3a** and **3b** in the carbonyl region show four strong bands, whose frequencies and intensities are virtually identical as expected for this genre of tetracarbonyl complexes. In addition to the well-separated resonances associated with the dppm ligand and ester groups, the ^{1}H NMR spectra display a doublet at δ 4.43 (J 5 Hz) for **3a** and 4.47 (J 8 Hz) for **3b** due to the C-H proton of the alkynyl ligand which couples to one of the phosphorus atoms of the dppm ligand. The hydride region in the ^{1}H NMR spectra shows a

doublet of doublets at δ -12.92 (J 9, 7 Hz) for **3a** and -12.93 (J 8, 12 Hz) for **3b**, each integrating for 1H, confirming the presence of an edge-bridging hydride ligand coupled toboth phosphorus atoms.The $^{31}P\{^{1}H\}$ NMR spectra recorded for **3a** and **3b** reveal two doublets [δ -2.3 and -11.9 (J 52 Hz) for **3a**; δ -2.1 and -11.8 (J 52 Hz) for **3b**], reaffirming the presence of inequivalent phosphorus atomsin the formulated structures of **3a** and **3b**.

Compounds **4a** and **4b** were characterized by analytical and spectroscopic methods, together with a single crystal X-ray diffraction analysis for **4b**. An ORTEP diagram ofthe molecular structure of **4b** is shown in Fig. 2 with selected bond distances and angles contained in the caption. Compound **4b** is electronically saturated and contains 48 valence electrons. The three osmium atoms display a scalene triangular array based on three distinctly different metal-metal bond lengths [Os(1)-Os(3) 2.7881(17), Os(1)-Os(2) 2.8729(19), Os(2)-Os(3) 3.0128(13) Å] and the dppm ligand bridges the Os(1)-Os(2) bond. The presence of seven terminal carbonyl ligands, two edge-bridging hydride ligands, and a face-capping DEAD ligand complete the ligand coordination sphere. The μ_3-DEAD ligand, which acts as a 4e donor, interacts with all three metal atoms through an $\eta^2(\pi)$-interaction between C(8)-C(9) and Os(1) [Os(1)-C(8) 2.251(8) and Os(1)-C(9) 2.060(7) Å] and through two formal Os-C σ-bonds to Os(2) and Os(3) [Os(2)-C(8) 2.153(8) and Os(3)-C(9) 2.063(8) Å]. The C(8)-C(9) bond distance in **4b** [1.408(10)] compares well to the C-C bond distance of 1.40(2)Å in the related alkyne-substituted cluster $Os_3(CO)_{10}(\mu_3\text{-}\eta^2;\eta^1;\eta^1\text{-DMAD})$ [39]. The two Os-P bond distances are nearly equal in length [Os(1)-P(1) 2.355(3), Os(2)-P(2) 2.340(2) Å] and comparable to the Os-P distances in the parent cluster **1** [2.336(5) and 2.337(5) Å] [1a]. The hydrides in **4b** could not be located from the structural studies, but are assumed to span Os(1)-Os(2) and Os(2)-Os(3) edges based on the disposition of the ancillary ligands about the three osmium centers.

Place Figure 2 Here

The spectroscopic recorded for **4b** are consistent with the solid-state structure. Given the similarity of the IR and NMR data of **4a** and **4b**, we conclude that these products are isostructural. The spectroscopic data for **4a** and **4b** are summarized in the experimental section.

Important features displayed by both products include two distinct hydride resonances that appear as a triplet and doublet. The former represents the hydride that shares the Os-Os edge with the bridging dppm ligand while the doublet is assigned to an adjacent Os-Os bond whose splitting is attributed to the vicinal phosphorus atom of the dppm ligand. The observed $^{2}J_{PH}$ coupling in the latter hydride confirms that the hydrides are non-fluxional under these conditions. Finally, the two doublets recorded in the ^{31}P NMR spectrum for the dppm ligand in each product are consistent with the formulated structure.

*3.2. Reactions of $Os_3(CO)_8(\mu$-dppf$)(\mu$-H$)_2$ (**2**) with DMAD and DEAD*

Two sets of new triosmium complexes, $Os_3(CO)_8(\mu$-dppf$)(\mu$-$\eta^2;\eta^1$-$RO_2CCHCCO_2R)(\mu$-H) (**5a**,R = Me,30%; **5b**, R = Et, 46%) and $Os_3(CO)_7(\mu$-dppf$)(\mu_3$-$\eta^2;\eta^1;\eta^1$-$RO_2CCCCO_2R)(\mu$-H$)_2$ (**6a**, R = Me, 26% **6b**, R = Et, 63%), were obtained when **2** was reacted with DMAD and DEAD, respectively, in refluxing benzene. Scheme 2 shows these reactions leading to the new triosmium clusters **5a**,**b** and **6a**,**b**.

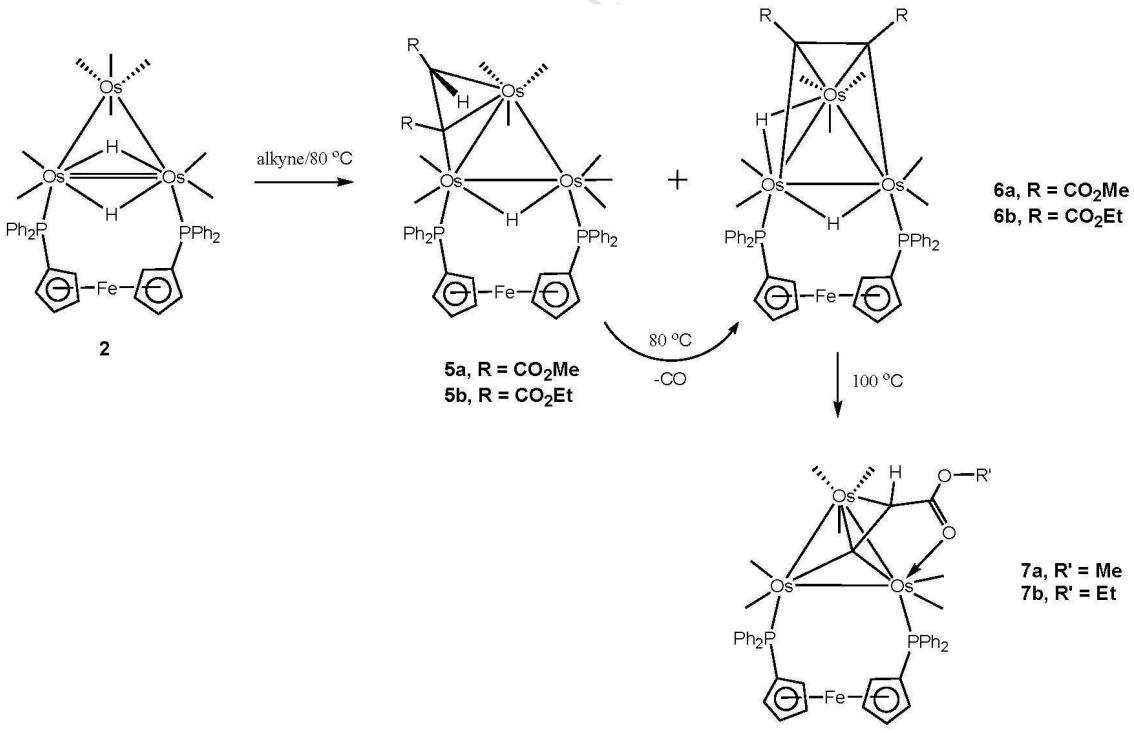

Scheme 2

Clusters **5a** and **5b** have been characterized by a combination of IR, and ^{1}H and $^{31}P\{^{1}H\}$ NMR spectroscopy, and the solid-state structure of **5a** has been established by single-crystal X-ray diffraction analysis. The molecular structure of **5a**, which is depicted in Fig. 3 and whose caption includes pertinent bond distances and bond angles, confirms the formal insertion of the alkyne into one of the hydride bonds in cluster **1** to yield an edge-bound alkenyl moiety. The closed triangular array of osmium atoms exhibitsthree distinctly different metal-metal bond lengths that range from 2.8156(5) Å [Os(1)-Os(3)] to 3.1191(5) Å [Os(1)-Os(2)] with a mean distance of 2.9514 Å. There are eight terminal carbonyl groups in **5a** and one of the CO groups at the $Os(CO)_4$ center in **1** has migrated to the adjacent Os(2) atom in **5a**. The dppf ligand bridges the Os(1)-Os(2) edge, and while the position of the hydride ligand in **5a** could not be located crystallographically, its association with the Os(1)-Os(2) edge is confirmed 1) by the disposition of the ancillary ligands about this Os-Os bond and 2) the fact that it is split into a triplet due to equal coupling with both phosphorus atoms of the dppf ligand [40]. The μ-$MeO_2CCHCCO_2Me$ ligand asymmetrically spans the Os(1)-Os(3) edge and displays a formal σ bond to Os(1) [Os(1)-C(9) 2.097(9) Å] and a π-bond interaction to Os(3) [Os(3)-C(9) 2.212(8) Å, Os(3)-C(10) 2.274(9) Å]. The σ-η^2vinyl-type interaction observed here is in keeping with the bond lengths found in other trimetallic systems with similar alkyne-derived ligands [41, 42]. The bridging alkenyl ligand acts as a 3e electron donor, and theπ-coordinated C(9)-C(10) double bond [1.453(13) Å]is elongated ca. 0.1 Å with respect to a free C=C double bond of an alkene.

Place Figure 3 Here

The recorded IR spectra in the ν(CO) region for **5a** and **5b** are similar, and the two clusters are assumed to be isostructural with respect to the distribution of their ligands about the Os_3 framework. Aside from the phenyl, cyclopentadienyl and $RO_2CCHCCO_2R$ (R = Me, Et) proton resonances in the ^{1}H NMR spectra, the hydride region of each product exhibits a triplet and a doublet of doublets at δ –17.67 (major) and –17.81 (minor) for **5a** and δ –17.69 (major) and –17.76 (minor) for **5b**, respectively, suggesting that each cluster exists as two isomers in solution. The existence of isomers is mirrored in the $^{31}P\{^{1}H\}$ NMR spectra of **5a** and **5b** based

on two sets of singlets for the inequivalent phosphorus atoms, as summarized in the experimental section.

The possible composition of the **5a** isomers was investigated by DFT, and here we employed the X-ray diffraction structure of **5a** as our starting point. Geometry optimization of **5a** using an ancillary dppf-Me_4 ligand furnished species **C** whose structure is shown in Fig. 4. The calculated structure for **C** shows good agreement with the solid-state structure of **5a** and reinforces the proposed location of the edge-bridging hydride across the dppf-Me_4-bridged Os-Os edge. We also optimized the structures of the starting cluster **2** (species **A**) and DMAD (species **B**) in order to evaluate the thermodynamics for the formation of **C**. The reaction of **A** with **B** to give **C** is exergonic, and the product lies 19.7 kcal/mol below the reactants. The potential energy (ΔG) surface for the reaction is shown in Fig. 5. Species **C_alt** was confirmed as the minor component of the isomers that constitute **5a**, and the main difference between **C** and **C_alt** concerns the disposition of the cyclopentadienyl rings of the dppf-Me_4 ligand relative to the metallic plane. We have described a similar torsional motion of the cyclopentadienyl ligands in the parent cluster **2** in our earlier report [13]. The free energy difference between the two species is small (ΔG = 0.7 kcal/mol) and favors **C**. The computed K_{eq} value of 0.30 for the **C**⇌ **C_alt** is somewhat greater than the experimentally found value of 0.53 for the isomer pair. This difference between the measured value of K_{eq} (0.53) and the computed value (0.30) can be attributed to the fact that DFT calculations were performed in the gas phase and no solvent correction has been applied.

Place Figures 4 and 5 Here

Independent control experiments established that compounds **5a**,**b** are precursors to **6a**,**b**. Thermolysis of **5a** and **5b** cluster in refluxing toluene leads to CO loss and the formation of the corresponding product **6a** and **6b**, respectively. This conversion of alkenyl complexes (**5a,b**) to alkyne and hydride complexes (**6a,b**) is quite unusual as normally an alkyne inserts into the metal-hydride bond to give an alkenyl complex [20, 21]. However, an alkyne-hydride intermediate has been proposed to form during α-β isomerisation of alkenyl ligands at binuclear

centers via this kind of conversion (Scheme 3) [43, 44]. The only difference between the two systems is that the alkenyl to alkyne conversion is reversible during α-β isomerisation of alkenyls at the binuclear centers, whereas the alkyne is 'trapped' here due to loss of CO which requires a change in coordination mode of the alkyne to preserve the EAN count of 48 at the trinuclear centers.

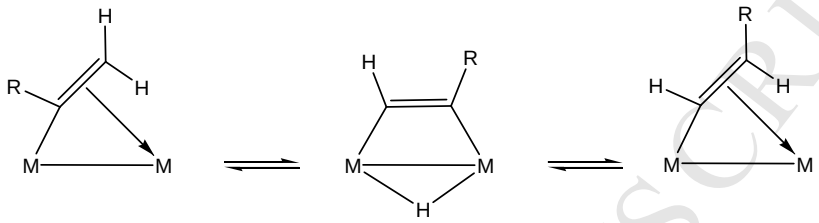

Scheme 3.

Both **6a** and **6b** were isolated by chromatography and structurally characterized by X-ray crystallography. The molecular structures of **6a** and **6b** are depicted in Figs. 6 and 7, respectively. Compounds **6a** and **6b** consist of a closed triangular array of osmium atoms whereone of the polyhedral faces is capped by the alkyne ligand. The transformation from **5a**,**b** to **6a**,**b** confirms that the original edge-bridging alkenyl moiety undergoes a C-H bond activation during the reaction. The Os-Os bond common to the bridging dppf and hydride ligands [Os(1)-Os(2) 3.0719(6) Å for **6a**; Os(1)-Os(3) 3.0685(6) Å for **6b**] is longer than the other hydride-bridged Os-Os edge [Os(2)-Os(3) 2.8726(17) Å for **6a**;and Os(2)-Os(3) 2.8649(5) for **6b**]. The mean Os-Os bond distance in **6a** and **6b** is similar to that in **4b**. The coordinated alkyne in each product displays the expected σ,π model of ligand bonding where the Os-C distances for the σ bonds [Os(1)-C(11) 2.080(3) Å, Os(2)-C(8) 2.129(3) Å for **6a**; Os(1)-C(9) 2.084(3) Å, Os(3)-C(8) 2.146(3) Å for **6b**] are shorter than the associated Os-C π distances [Os(3)-C(8) 2.215(3) Å, Os(3)-C(11) 2.300(3) Å for **6a**; Os(2)-C(8) 2.235(3) Å, Os(2)-C(9) 2.308(3) Å for **6b**].The Os-P bond distances [Os(1)-P(2) 2.3437(8) Å, Os(2)-P(1) 2.3588(8) Å for **6a**; Os(1)-P(1)2.3498(10)Å, Os(3)-P(2) 2.3653(8) Å for **6b**] are similar to those distances found in the starting cluster **2** [13]. Both products are electron precise based on an electron count of 48 valence electrons.

Place Figures 6 and 7 Here

The IR spectra recorded for clusters **6a** and **6b** are identical in the terminal ν(CO) region and consistent with a common distribution of the ancillary ligands about each Os_3 polyhedron. Both clusters exist as a mixture of two isomers in $CDCl_3$ solution that are in rapid equilibrium. Since the NMR spectral data for the two clusters are similar in nature, we will only discuss the properties of **6a** in detail. The ^{31}P NMR spectrum of **6a** at room temperature reveals a broad resonance at δ -3.8 that is barely distinguishable from the baseline, and the visible absence of inequivalent phosphorus nuclei confirms the existence of a fluxional process. The exchange process creates a time-average environment for the dppf ligand and the nature of the broadened ^{31}P resonance allows us to approximate the temperature of coalescence (T_c) as 298 K. The ^{1}H NMR spectrum exhibits two triplets at δ -16.65 and -19.80 at 298 K whose splitting pattern indicates that the two hydrides are coupled to both phosphorus atoms of the dppf ligand. Identical splitting patterns for the hydrides signal a rapid exchange of the hydride associated with the Os-Os bond that is adjacent to the dppf-bridged Os-Os bond. While a triplet resonance is expected for the hydride that shares the Os-Os edge common to the dppf ligand, the second hydride is situated asymmetrically to the dppf ligand (see the solid-state structure) and should display either a doublet or a doublet of doublets instead of a triplet resonance. Figs. 8 and 9 show the VT ^{31}P and ^{1}H NMR spectra, respectively recorded for cluster **6a** over the temperature range 318-233 K.

Place Figures 8 and 9 Here

Lowering the temperature to 233 K leads to two sharp singlets at δ -9.7 and 3.2 in the $^{3}1P$ NMR spectrum, and while the high-field triplet at δ -19.80 does not exhibit any appreciable change in the ^{1}H NMR spectra as the temperature is lowered, the triplet at δ -16.65 transforms to a doublet with J_{PH} = 20 Hz as the slow-exchange limit is approached. These data support a fluxional process that serves to equilibrate the latter hydride between the two Os-Os edges that are not bridged by the dppf ligand. Hydride mobility about polynuclear metal clusters is a well-

established phenomenon [45]. At 233 K, two distinct ^{31}P and ^{1}H resonances are expected, with one hydride effectively coupled to only one of the ^{31}P centers. The $\Delta G^{\ddagger}$ value for the equilibration of the hydride between adjacent Os-Os vectors is estimated as 11.9 kcal/mol based on a separation frequency of the ^{31}P resonances ($\Delta\nu$ = 2363 Hz) and a T_c of 298 K [46]. Scheme 4 illustrates the hydride exchange process that is consistent with the VT NMR data.

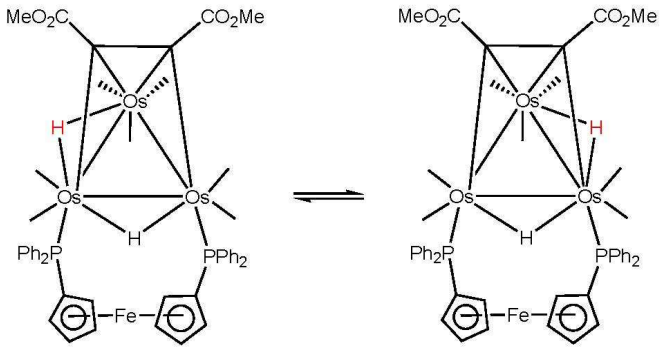

6a **6a**

Scheme 4

To better understand the observed ligand fluxionality in **6a**, we have investigated different possible hydride exchange schemes employing species **D** as a starting point. Equilibration of the hydride between the two non-dppf supported Os-Os bonds proceeds via the transition state **TSDD_alt** that contains a triply bridged hydride ligand (Chart). The computed $\Delta G^{\ddagger}$ value for the forward motion of the hydride is 7.2 kcal/mol in agreement with the experimentally estimated value for hydride fluxionality. The motion exhibited by the migratory hydride is analogous to the windshield-wiper effect displayed by related ligands across the polyhedral face of other metal clusters [45b,e, 47]. The product of hydride transit is **D_alt**, and it lies 1.1 kcal/mol lower in energy than **D** due to slight differences in the disposition of the dppf-Me_4 and carbonyl ligands about the cluster. Under conditions of rapid exchange, the hydride would exhibit a time-average environment between the Os-Os bonds and display mutual coupling to both phosphines, giving rise to the observed triplet resonance at δ -16.65.

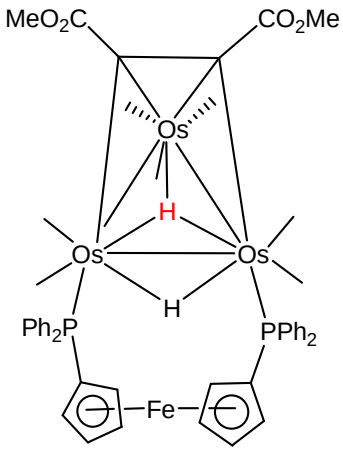

Chart

*3.3. Carbon-carbon bond cleavage of the coordinated alkyne ligand in **6a** and **6b***

The cleavage of carbon-carbon bonds is a potentially useful way of generating reactive organic fragments at a metal center [48]. To this end, we have been exploring the reactions of coordinated alkynes at different metal clusters and can report that the coordinated alkyne ligands in **6a**,**b** yield new clusters containing a vinylidene moiety when heated at elevated temperatures. Thermolysis of **6a** and **6b** in toluene at 110 °C, followed by the usual chromatographic separation, afforded $Os_3(CO)_7(\mu\text{-dppf})(\mu_3\text{-}\eta^2;\eta^1;\kappa^1\text{-}CCHCO_2R)$ (**7a**, R = Me, 50%; **7b**, R = Et, 48%) (Scheme 2). While we have not been able to identify the missing alkyne-derived atoms in these reactions, we can confirm that corresponding formates HCO_2Me and HCO_2Et are not observed in those reactions that are monitored by NMR. The cluster products are relatively stable under the reaction conditions and show no evidence of decomposition when heated in refluxing toluene over the course of several hours. Compounds **7a** and **7b** have been characterized spectroscopically in solution and by X-ray diffraction analysis in the case of **7b**, whose structure is shown in Fig. 10.

Place Figure 10 Here

The Os-Os bond distances in **7b** range from 2.7740(11) Å [Os(1)–Os(3)] to 3.0481(11) Å [Os(1)–Os(2)], leading to a triangular array of osmium similar in nature to that found in clusters **6a** and **6b**. The most noteworthy feature in **7b** is the face-capping $CCHCO_2Et$ ligand that derives from the coordinated DEAD ligand in **6b**. The $CCHCO_2Et$ ligand, which functions as a 6e donor, is coordinated to the cluster in a μ_3-η^2;η^1;κ^1 fashion, where the C(8) and C(9) atoms exhibit Os-C distances consistent with a σ,π model of bonding common to other vinylidene ligands [49]. Here the two σ bonds are represented by the Os(1)-C(8) [2.131(11) Å] and Os(2)-C(8) [1.963(15) Å] vectors and the π interaction is defined by Os(3)-C(8) [2.187(12) Å] and Os(3)-C(9) [2.331(14) Å] vectors. There is also an additional donation of 2e to the Os(1) center from the O(8) carbonyl oxygen of the ester moiety. Cluster **7b** contains 48 valence electrons and be viewed as an electron-precise cluster containing three metal-metal bonds. The dppf ligand bridges the Os(1) and Os(2) centers, and of the seven terminal carbonyl groups, three are located at the Os(3) center with the remaining four CO groups distributed pair wise at the other two metal centers.

The spectroscopic data recorded for **7a** is consistent with the formulated structure containing an ancillary $CCHCO_2Me$ vinylidene ligand, and this premise is underscored by the near identical IR spectra displayed by **7a** and **7b**. In addition to the phenyl proton resonances in the aromatic region, the ^{1}H NMR spectrum of each product also contains nine equal intensity singlets [δ 5.33, 5.04, 4.32, 4.25, 4.09, 3.81, 3.73, 3.70, 3.33 for **7a** and δ 5.33, 5.28, 5.04, 4.32, 4.24, 4.10, 3.81, 3.70, 3.34 for **7b**] ascribed to the eight distinct cyclopentadienyl protons and one unique vinylic proton. The methyl group in the $CCHCO_2Me$ moiety appears as a singlet at δ 2.83 in **7a**, while the ethyl group associated with the $CCHCO_2Et$ ligand exhibits a triplet at δ 0.96 for the methyl group and two multiplets at δ 3.19 and 2.93, the latter two assigned to the diastereotopic methylene hydrogens. Each cluster exhibits a pair of ^{31}P singlets [δ 14.5 and 7.1 for **7a**; δ 14.2 and 6.8 for **7b**] due to the nonequivalent ^{31}P nuclei.

4. Conclusions

The reactions of the unsaturated triosmium clusters $Os_3(CO)_8(\mu\text{-dppm})(\mu\text{-H})_2$ (**1**) and $Os_3(CO)_8(\mu\text{-dppf})(\mu\text{-H})_2$ (**2**) with activated alkynes DMAD and DEAD are examined. Cluster **1**

reacts with these alkynes to furnish the dinuclear $Os_2(CO)_4(\mu\text{-dppm})(\mu\text{-}\eta^2;\eta^1;\kappa^1\text{-}RO_2CCCHCO_2R)(\mu\text{-H})$ (**3a**, R = Me; **3b**, R = Et) and the trinuclear $Os_3(CO)_7(\mu\text{-dppm})(\mu_3\text{-}\eta^2;\eta^1;\eta^1\text{-}RO_2CCCCO_2R)(\mu\text{-H})_2$ (**4a**, R = Me; **4b**). In contrast, no cluster fragmentation has been observed when **2** is allowed to react with these alkynes under comparable conditions, instead yields the trinuclear $Os_3(CO)_8(\mu\text{-dppf})(\mu\text{-}\eta^2;\eta^1\text{-}RO_2CCHCCO_2R)(\mu\text{-H})$ (**5a**, R = Me; **5b**, R = Et) and $Os_3(CO)_7(\mu\text{-dppf})(\mu_3\text{-}\eta^2;\eta^1;\eta^1\text{-}RO_2CCHCCO_2R)(\mu\text{-H})_2$ (**6a**, R = Me; **6b**, R = Et). Independent control experiments reveal that **5a** and **5b** serve as precursors to **6a** and **6b**, respectively. These data are interesting insomuch that the latter products are not formed as the initial products of ligand substitution and that alkyne insertion into an Os-H bond precedes the formal π coordination of the alkyne by the cluster in the present examples. The computed thermodynamics for the reaction reinforce this claim. However, this observation strengthened the reversible alkenyl to alkyne and hydride conversion proposed for the α-β isomerisation of alkenyl ligands at binuclear centers [43, 44]. Both **5a** and **5b** exist as a pair of isomers in solution due to a torsional rotation within the cyclopentadienyl rings of the dppf ligandwith respect to the osmium triangle. This fluxionality has been computationally evaluated for **5a** and the energy difference between the two isomers is small (ΔG = 0.7 kcal/mol). CO loss in **5a** and **5b** is facile, and the accompanying unsaturated clusters facilitate the C-H bond activation of the alkenyl moiety to yield the π-coordinated clusters **6a** and **6b**. Thermolysis of the latter two clusters leads to alkyne activation and formation of the vinylidene-substituted clusters **7a** and **7b**. The alkyne activation observed here is related to the carbon-carbon cleavage reported for triruthenium compound $[(\eta^5\text{-}C_5Me_5)Ru]_3(\mu\text{-H})_3(\mu_3\text{-H})_2$ in its reaction with methylmethacrylate to furnish $[(\eta^5\text{-}C_5Me_5)Ru]_3(\mu_3\text{-CH=CCO}_2Me)(\mu_3\text{-CH})(\mu\text{-H})_2$ together with 2 equivalents of 2-methylbutanoic acid [48e]. In contrast, formation of such vinylidene-substituted clusters via alkyne activation was not observed upon heating of **4a** and **4b**. Overall, the present work shows that the flexibility of substituted-diphosphine plays key role in the reactivity of unsaturated $Os_3(CO)_8(\mu\text{-diphosphine})(\mu\text{-H})_2$ towards alkynes. Experiments designed to elucidate the mechanism of carbon-carbondouble bond cleavage and further investigation using a wider range of alkynes are underway, and the results willbe reported in due course.

5. Acknowledgments

Part of this work was carried out by SEK at the University of Göttingen, who acknowledges the von Humboldt Foundation for providing research support during his stay at the University of Göttingen. MGR thanks the Robert A. Welch Foundation (grant B-1093) for financial support and acknowledges computational resources through UNT's High-Performance Computing Services and CASCaM. We also thank Prof. Michael B. Hall (TAMU) for providing us a copy of his *JIMP2* program.

6. Supplementary data

Figs. S1-S3, showing CH_2Cl_2 proton resonance in the ^1H NMR spectrum of compounds **3a**, **5a** and **7b**, can be found in Electronic Supplementary Information (ESI). Crystallographic data for the structural analyses have been deposited with the Cambridge Crystallographic Data Centre. CCDC 1517049 (for **3a**), CCDC 1517050 (for **4b**), CCDC 1517051 (for **5a**), CCDC 1517052 (for **6a**), CCDC 1517053(for **6b**) and CCDC 1517054(for **7b**) contain supplementary crystallographic data for this paper. These data can be obtained free of charge from the Director, CCDC, 12 Union Road, Cambridge, CB2 1 EZ, UK (fax: +44-1223-336033; Email: deposit@ccdc.cam.ac.uk or www: http://www.ccdc.ac.uk). Atomic coordinates for all optimized structures reported here are available from MGR upon request.

References

[1] J.A. Clucas, M.M. Harding, A.K. Smith, J. Chem. Soc.,Chem. Commun. (1984) 949.

[2] J.A. Clucas, M.M. Harding, A.K. Smith, J. Chem. Soc., Chem. Commun. (1985) 1280.

[3] (a) J.A. Clucas, M.M. Harding, A.K. Smith, J. Chem. Soc., Chem. Commun. (1987) 1829; (b) M.P. Brown, P.A. Dolby, M.M. Harding, A.J. Mathews, A.K. Smith, D. Osella, M. Arbrun, R. Gobetto, P.R. Raithby, P. Zanello, J. Chem. Soc. Dalton Trans. (1993) 827; (c) M.P. Brown, P.A. Dolby, M.M. Harding, A.J. Mathews, A.K. Smith, J. Chem. Soc., Dalton Trans. (1993) 1671; (d) M.M. Harding, B.A. Kariuki, J. Mathews, A.K. Smith, P. Braunstein, J. Chem. Soc., Dalton Trans. (1994) 33.

[4] A. Pöe, V.C. Sekhar, J. Am. Chem. Soc. 106 (1984) 5034.

[5] R.A. Bartlett, C.D. Cardin, D.J. Cardin,G.A. Lawless, J.M. Power, P.P. Power, J. Chem. Soc., Chem.Commun. (1988) 312.

[6] S.E. Kabir, G. Hogarth, Coord. Chem. Rev. 253 (2009) 1285.

[7] (a) A.J. Deeming, S. Donovan-Mtunzi, S.E. Kabir, J. Organomet. Chem. 276 (1984) C65; (b) A.J. Deeming, S. Donovan-Mtunzi, S.E. Kabir, J. Organomet. Chem. 333 (1987) 253; (c) A.J. Deeming, S. Donovan-Mtunzi, K.I. Hardcastle, S.E. Kabir, K. Henrick, M. McPartlin, J. Chem. Soc., Dalton Trans. (1988) 579; (d) A.J. Deeming, K.I. Hardcastle, S.E. Kabir, J. Chem. Soc., Dalton Trans. (1988) 827; (2011) 1432.

[8] (a) K.A. Azam, M.B. Hursthouse, Md.R. Islam, S.E. Kabir, K.M.A. Malik, R. Miah, C. Sudbrake, H. Vahrenkamp, J. Chem. Soc. Dalton Trans. (1998) 1097; (b) K.A. Azam, M.B. Hursthouse, S.E. Kabir, K.M.A. Malik, M.A. Mottalib, J. Chem. Crystallogr. 29 (1999) 813; (c) S.M.T. Abedin, K.I. Hardcastle, S.E. Kabir, K.M.A. Malik, Md. A. Mottalib, E. Rosenberg, M.J. Abedin, Organometallics 19 (2000) 5623; (d) S.E. Kabir, K.M.A. Malik, M.E. Molla, Md. A. Mottalib, J. Organomet. Chem. 616 (2000) 157; (e) S.E. Kabir, K.M.A. Malik, C.A. Johns, Md. A. Mottalib, J. Organomet. Chem. 625 (2001) 112; (f) A.J. Deeming, M.M. Hasan, S.E. Kabir, E. Nordlander, D.A. Tocher, Dalton Trans. (2004) 3709; (g) S.E. Kabir, N. Begum, Md.M. Hasan, Md.I. Hyder, H. Nur, D.W. Bennett, T.A. Siddique, D.T. Haworth, E. Rosenberg, J. Organomet. Chem. 689 (2004) 1569 (h) S.E. Kabir, Md. A. Miah, N.C. Sarker, G.M.G. Hossain, K.I. Hardcastle, D. Rokhsana, E. Rosenberg, J. Organomet. Chem. 690 (2005) 3044; (i) S.M. Azad, K.A. Azam, S.E. Kabir, M.S. Saha, G.M.G. Hossain, J. Organomet. Chem. 690 (2005) 4206;(j) M.R. Hassan, G. Hogarth, G.M.G. Hossain, S.E. Kabir, A.K. Raha, M.S. Saha, D.A. Tocher, Organometallics 26 (2007) 6473; (k) A.K. Raha, S. Ghosh, M.M. Karim, D.A. Tocher, A. Sharmin, E. Rosenberg, S.E. Kabir, J. Organomet. Chem. 693 (2008) 3613; (l) A.K. Raha, S. Ghosh, S.E. Kabir, B.K. Nicholson, D.A. Tocher, J. Organomet. Chem. 694 (2009) 752; (m) A.K. Raha, S. Ghosh, I. Hossain, S.E. Kabir, B.K. Nicholson, G. Hogarth, L. Salassa, J. Organomet. Chem. 696 (2011) 2153; (n) S. Ghosh, G. Hogarth, S.E. Kabir, A.K. Raha, M.G. Richmond, J.C. Sarker, J. Clust. Sci. 23 (2012) 781; (o) A.K. Raha, Md.N. Uddin, S. Ghosh, A.R. Miah, M.G. Richmond, D.A. Tocher, E. Nordlander, G. Hogarth, S.E. Kabir, J. Organomet. Chem. 751 (2014) 399.

[9] A.A. Koridze, S.A. Kuklin, N.A. Shtelzer, F.M. Dolgushin, M.G. Ezernitsjkaya, Russ. Chem. Bull. 57 (2008) 2194.

[10] B.F.G. Johnson, J. Lewis, D.A. Pippard, J. Chem. Soc. Dalton Trans. (1981) 407.

[11] S.-H. Huang, J.M. Keith, M.B. Hall, M.G. Richmond, Organometallics 29 (2010) 4041.

[12] J.C. Sarker, Kh.M. Uddin, Md.S. Rahman, S. Ghosh, T.A. Siddiquee, D.A. Tocher, M.G. Richmond, G. Hogarth, S.E. Kabir, Inorg. Chim. Acta 409 (2014) 320.

[13] N. Begum, U.K. Das, M. Hassan, G. Hogarth, S.E. Kabir, E. Nordlander, M.A. Rahman, D.A. Tocher, Organometallics 26 (2007) 6462.

[14] E.N. Ho, B.K. Hiu, W. Wong, J. Organomet. Chem. 637 (2001) 276.

[15] G. Hogarth, S.E. Kabir, E. Nordlander, Dalton Trans. 39 (2010) 6153.

[16] (a) S.E. Kabir, D.S. Kolwaite, E. Rosenberg, K.I. Hardcastle, W. Cresswell, J. Grindstaff, Organometallics 14 (1995) 3611; (b) M.J. Abedin, B. Bergman, R. Holmquist, R. Smith, E. Rosenberg, K.I. Hardcastle, J. Roe, V. Vazquez, C. Roe, S.E. Kabir, B. Roy, S. Alam, K.A. Azam, R. Duque, Coord. Chem. Rev. 190–192 (1999) 975.

[17] (a) H.D. Kaesz, S.A.R. Knox, J.W. Koepke, R.B. Saillant, J. Chem. Soc. Chem. Commun. (1971) 477; (b) A.J. Deeming, Adv. Organomet. Chem. 26 (1986) 1.

[18] (a) W.G. Jackson, B.F.G. Johnson, J.W. Kelland, J. Lewis, K.T. Schorpp, J. Organomet. Chem. 87 (1975) C27; (b) A.J. Deeming, S. Hasso, M. Underhill, J. Chem. Soc., Dalton Trans. (1975) 1614; (c) J.B. Keister, J.R. Shapley, J. Organomet. Chem. 85 (1975) C29 (d) M.R. Churchill, F.J. Hollander, J.P. Hutchinson, Inorg. Chem. 16 (1977) 2697; (e) R.B. Calvert, J.R. Shapley, J. Am. Chem. Soc. 99 (1977) 5225; (f) R.D. Adams, G. Chen, J.T. Tanner, Organometallics 9 (1990) 1530; (g) J.R. Shapley, Inorg. Chem. 21 (1982) 3295; (h) E. Sappa, A. Tirripicchio, A.M. Manotti Lanfredi, J. Organomet. Chem. 249 (1983) 391; (i) Z. Dawoodi, M.J. Mays, J. Chem. Soc., Dalton Trans. (1984) 1931; (j) E. Rosenberg, E. Anslyn, L. Milone, S. Aime, R. Gobetto, D. Osella, Gazz. Chim. Ital. 118 (1988) 299;(k) R. Gobetto, L. Milone, F. Reineri, L. Salassa, A. Viale, E. Rosenberg, Organometallics 21 (2002) 1919; (l) M.J. Stchedroff, V. Moberg, E. Rodriguez, A.E. Aliev, J. Boettcher, J.W. Steed, E. Nordlander, M. Monari, A.J. Deeming, Inorg. Chim. Acta 359 (2006) 926; (m) C.E. Cooke, M.C. Jennings, M.J. Katz, R.K. Pomeroy, J.A.C. Clyburne, Organometallics 27 (2008) 5777; (n) O.A. Kizas, S.Y. , D.Y. Antonov, I.A. Godovikov, E.V. Vorontsov, F.M. Dolgushin, M.G. Ezernitskaya, I.G.

Barakovskaya, New J. Chem. 33 (2009)1760; (o) J.A. Cabeza, I. del Rio, J.M. Fernandez-Colinas, E. Perez-Carreno, M.G. Sanchez-Vega, D. Vazquez-Garcia, Organometallics 29 (2010) 3828; (p) A. Gonzalez-Hernandez, S. Hernandez-Ortega, E. Gomez, J.M. Fernandez-G, J. Organomet. Chem. 696 (2011) 3436; (q) S.K. Brayshaw, L.P. Clarke, P. Homanen, O.F. Koentjoro, J.E. Warren, P.R. Raithby, Organometallics 30 (2011) 3955.

[19] (a) R. Noyori, Angew. Chem., Int. Ed. Engl.36 (1997) 285; (b) J.F. Knifton, J. Org. Chem.41 (1976) 2885;(c) D. Bingham, D.E. Webster,P.B. Wells, J. Chem. Soc.,Dalton Trans.(1974)1514; (d) D. Bingham, D.E. Webster,P.B. Wells, J. Chem. Soc.,Dalton Trans.(1974) 1519; (e) R. Cramer, J. Am. Chem. Soc.87 (1965) 4717; (f) I. Ojima,M. Eguchi, M. Tzamarioudaki, Comprehensive OrganometallicChemistry II, Pergamon, Oxford, 1995, vol. 12, ch. 2.

[20](a) E. Sappa, A. Tirripicchio, P. Braunstein, Chem. Rev. 83 (1983) 203; (b) D. Osella, P.R. Raithby, in I. Bernal (Ed.), Stereochemistry of Organometallic and Inorganic Compounds, Elsevier, Amsterdam, 1988, vol. 3.

[21] (a) Kh.M. Uddin, S. Ghosh, A.K. Raha, G. Hogarth, E. Rosenberg, A. Sharmin, K.I. Hardcastle, S. E. Kabir, J. Organomet. Chem. 695 (2010) 1435; (b) S. Ghosh, M.R. Al-Mamun, G.M.G. Hossain, S.E. Kabir, Inorg. Chim. Acta 378 (2011) 307.

[22] (a) A.J. Deeming, S.E. Kabir, J. Organomet. Chem. 340 (1988) 359; (b) M. Stchedroff, V.Moberg, E. Rodriguez, A.E. Aliev, J. Bottcher,J.W. Steed, E. Nordlander, M. Monari, A.J. Deeming, *Inorg. Chim.Acta* 359 (2006) 926.

[23] G.M. Sheldrick, SADABS Version 2.10 (University of Göttingen, 2003).

[24] Crystal Clear Software User's Guide, Molecular Structure Corporation, Rigaku Corporation,Japan, 1999, pp-1718-1725.

[25] CrysAlisPRO, Agilent Technologies UK Ltd, Yarnton, England.

[26] G.M. Sheldrick, Program for Crystal Structure Solution and Refinement Acta Cryst. A64 (2008) 112.

[27] L.J. Farrugia, J. Appl. Cryst. 45 (2012) 849.

[28] O.V. Dolomanov, L.J. Bourhis, R.J. Gildea, J.A.K. Howard, H. Puschmann, OLEX2: A complete structure solution, refinement, and analysis program. J. Appl. Cryst. 42 (2009) 339.

[29] M.J. Frisch, G.W. Trucks, H.B. Schlegel, G.E. Scuseria, M.A. Robb, J.R. Cheeseman, G. Scalmani, V. Barone, B. Mennucci, G.A. Petersson, H. Nakatsuji, M. Caricato, X. Li, H.P. Hratchian, A.F. Izmaylov, J. Bloino, G. Zheng, J.L. Sonnenberg, M. Hada, M. Ehara, K. Toyota, R. Fukuda, J. Hasegawa, M. Ishida, T. Nakajima, Y. Honda, O. Kitao, H. Nakai, T. Vreven, J.A. Montgomery, Jr., J.E. Peralta, F. Ogliaro, M. Bearpark, J.J.. Heyd, E. Brothers, K.N. Kudin, V. N. Staroverov, R. Kobayashi, J. Normand, K. Raghavachari, A. Rendell, J.C. Burant, S.S. Iyengar, J. Tomasi, M. Cossi, N. Rega, J.M. Millam, M. Klene, J.E. Knox, J.B. Cross, V. Bakken, C. Adamo, J. Jaramillo, R. Gomperts, R.E. Stratmann, O. Yazyev, A.J. Austin, R. Cammi, C. Pomelli, J.W. Ochterski, R.L. Martin, K. Morokuma, V.G. Zakrzewski, G.A. Voth, P. Salvador, J.J. Dannenberg, S. Dapprich, A.D. Daniels, O. Farkas, J.B. Foresman, J.V. Ortiz, J. Cioslowski, D.J. Fox, Gaussian 09, Revision A.02, Gaussian, Inc., Wallingford CT, 2009.

[30] A.D. Becke, J. Chem. Phys. 98 (1993) 5648.

[31] C. Lee, W. Yang, R.G. Parr, Phys. Rev. B 37 (1988) 785.

[32] (a) M. Dolg, U. Wedig, H. Stoll, H. Preuss, J. Chem. Phys. 86 (1987) 866; (b) S.P. Walch, C.W. Bauschlicher, J. Chem. Phys. 78 (1983) 4597.

[33] (a) G.A. Petersson, A. Bennett, T.G. Tensfeldt, M.A. Al-Laham, W.A. Shirley, J. Mantzaris, J. Chem. Phys. 89 (1988) 2193; (b) G.A. Petersson, M.A. Al-Laham, J. Chem. Phys. 94 (1991) 6081.

[34] C.J. Cramer, Essentials of Computational Chemistry, 2nd Ed.; Wiley: Chichester, UK, 2004.

[35] (a) JIMP2, version 0.091, a free program for the visualization and manipulation of molecules: M.B. Hall, R.F. Fenske, Inorg. Chem. 11 (1972) 768; (b) J. Manson, C.E. Webster, M.B. Hall, Texas A&M University, College Station, TX, 2006: http://www.chem.tamu.edu/jimp2/index.html.

[36] M.R. Burke, J. Takats, J. Organomet. Chem. 439 (1986) 325.

[37] G. Hogarth, M.H. Lavender, Inorg. Chim. Acta 409 (1994) 3390.

[38] M.R. Burke, J. Takats, F.-W. Grevels, J.G.A. Reuvers, J. Am. Chem. Soc. 105 (1983) 4092.

[39] A.J. Deeming, A.M. Senior, J. Organomet. Chem. 439 (1992) 177.

[40] M.R. Churchill, In Transition Metal Hydrides;Bau, R. Ed.; Advances in Chemistry Series 167; American Chemical Society: Washington, DC, 1978.

[41] (a) J.A. Cabeza, J.M. Fernandez-Colinas, A. Llamazares, V. Riera, S. Garcia-Grande, J.F. Van der Maelen, Organometallics, 13 (1994) 4352; (b) N. Lugan, F. Laurent, G. Lavigne, T. Newcomb, E.W. Liimatta, J. Bonnet, J. Am. Chem. Soc. 112 (1990) 8607; (c) P. Nombel, N. Lugan, F. Mulla, G. Lavigne, Organometallics, 13 (1994) 4673.

[42] J.A. Cabeza, I. del Rio, J.M. Fernandez-Colinas, V. Riera, Organometallics, 15 (1996) 449.

[43] (a) S. Doherty, G. Hogarth, Chem. Commun. (1998) 1815; (b) M.K. Anwar, G. Hogarth, O.S. Senturk, W. Clegg, S. Doherty, M.R.J. Elsegood, J. Chem. Soc., Dalton Trans. (2001) 341.

[44] (a) Y. Gao, M.C. Jennings, R.J. Puddephatt, Dalton Trans. (2003) 261; (b) M.A. Alvarez, M.E. Garcia, D. Garcia-Vivo, M.A Ruiz, M.F. Vega, M. Fernanda, Dalton Trans. 45 (2016) 5274.

[45] (a) J.B. Keister, U. Frey, D. Zbinden, A.E. Merbach, Organometallics 10 (1991) 1497; (b) M. Day, D. Eepitia, K.I. Hardcastle, S.E. Kabir, E. Rosenberg, R. Gobetto, L. Milone, D. Osella, Organometallics 10 (1991) 3550; (c) L.R. Nevinger, J.B. Keister, Organometallics 9 (1990) 2312; (d) E. Rosenberg, Polyhedron 8 (1989) 383; (e) E. Rosenberg, R. Kumar, J. Clust. Sci. 25 (2014) 239.

[46] (a) Here the free energy of activation has been computed using the Eyring equation: $\Delta G^{\ddagger} = RT_c[\ln(k_BT_c/hk_c)]$, where the physical constants k_B and h have their normal meanings and T_c and k_c represent the coalescence temperature and the rate constant at coalescence. The value for k_c has been estimated as a function of $\Delta\nu$ according to the equation: $k_c = (0.5)^{1/2}\pi\Delta\nu$; (b) J.W. Akitt, B.E. Mann, NMR and Chemistry, Stanley Thornes, UK, 2000.

[47] (a) M.J. Hossain, S. Rajbangshi, M.M.M. Khan, S. Ghosh, G. Hogarth, E. Rosenberg, K.I. Hardcastle, M.G. Richmond, S.E. Kabir, J. Organomet. Chem. 767 (2014) 185; (b) M.K. Hossain, S. Rujbangshi, A. Rahaman, M.A.H. Chowdhury, T.A. Siddiquee, S. Ghosh, M.G. Richmond, E. Nordlander, G. Hogarth, S.E. Kabir, J. Organomet. Chem. 760 (2014) 231.

[48] (a) R.D. Adams, X. Qu, W. Wu, Organometallics 14 (1995) 1377; (b) A.J. Deeming, M.S.B. Felix, D. Nuel,Inorg. Chim. Acta 213 (1993) 3; (c) M. Murakami, T. Matsuda, Chem. Commun. 2011, 47, 1100; (d)M. Tobisub, N. Chatani, Chem. Soc. Rev. 37 (2008) 300; (e)T. Takemori, A. Inagaki, H. Suzuki, J. Am. Chem. Soc.123 (2001)1762.

[49] (a) E. Delgado, J.C. Jeffery, F.G.A. Stone, J. Chem. Soc., Dalton Trans. (1986) 2105; (b) A.S. Batsanov, V.G. Andrianov, Y.T. Struchkov, A.A. Koridze, O.A. Kizas, N.E. Kolobova, J.

Organometal. Chem. 329 (1987) 401; (c) M.K. Alami, F. Dahan, J.-J. Bonnet, R. Mathieu, Organometallics 7 (1988) 1391; (d) D.E. Fogg, S.A. MacLaughlin, K. Kwek, A.A. Cherkas, N.J. Taylor, A.J. Carty, J. Organomet. Chem. 352 (1988) C17.

Table 1. Crystallographic data and structure refinement for **3a**, **4b**, **5a**, **6a**, **6b**, and **7b**.

Compound	**3a**	4**b**	**5a**
Empirical formula	$C_{37}H_{34}Cl_4O_8Os_2P_2$	$C_{40}H_{32}O_{11}Os_3P_2$	$C_{49}H_{36}Cl_2FeO_{12}Os_3P_2$
Formula weight	1190.78	1321.20	1576.07
Temperature (K)	150(2)	293(2)	150(2)
Wavelength (Å)	0.71073	0.71075	1.5418
Crystal system	Orthorhombic	Triclinic	Triclinic
Space group	*Pbca*	*P*-1	*P*-1
a (Å)	18.641(3)	10.432(7)	11.2207(5)
b (Å)	18.670(3)	11.409(7)	11.8314(5)
c (Å)	23.229(4)	19.735(12)	21.2863(8)
α (°)	90	101.741(5)	79.282(3)
β (°)	90	98.724(7)	83.351(4)
γ (°)	90	109.420(2)	69.020(4)
Volume ($Å^{-3}$)	8085(2)	2107(2)	2588.79(19)
Z	8	2	2
Calculated density (mg/m^3)	1.957	2.083	2.022
Absorption coefficient (mm^{-1})	6.673	9.157	17.793
F(000)	4560	1236	1488
Crystal size (mm)	0.20 x 0.08 x 0.03	0.23x 0.18 x 0.09	0.32 x 0.28 x 0.23
θ range for data collection (°)	2.80 to 28.30	1.08 to 27.59	4.05 to 50.00
Reflections collected	65432	21038	11409
Independent reflections(R_{int})	9667[0.1263]	9641 [0.0453]	5305 [0.0194]
Data / restraints / parameters	9667/0/448	9641/0/500	5305/4/624
Goodness-of-fit on F^2	0.904	1.087	1.103
Final R indices [$I > 2\sigma(I)$]	R_1 = 0.0551, wR_2 = 0.1141	R_1 = 0.0450, wR_2 = 0.0918	R_1 = 0.0327, wR_2 = 0.0884
Largest diff. peak/ hole ($e.Å^{-3}$)	2.443 and -3.258	1.403 and -1.980	1.491 and -0.965

Table 1. (*Continued*)

6a	**6b**	**7b**
$C_{47}H_{36}FeO_{11}Os_3P_2$	$C_{49}H_{40}FeO_{11}Os_3P_2$	$C_{47}H_{35}Cl_2FeO_9Os_3P_2$
1465.15	1493.20	1503.04
105(4)	150(2)	150(2)
0.71073	0.71073	1.5418
Monoclinic	Monoclinic	Orthorhombic
$P2_1/c$	*$P2_1/n$*	*Pca21*
15.5899(3)	11.191(5)	16.5301(8)
11.7929(2)	19.701(5)	11.4243(4)
24.9054(5)	22.186(5)	25.4610(14)
90	90	90
102.090(2)	94.631(5)	90
90	90	90
4477.30(16)	4875(3)	4808.2(4)
4	4	4
2.174	2.034	2.076
8.937	8.209	19.070
2760.0	2824	2828
0.24 x 0.16 x 0.1	0.23 x 0.17 x 0.13	0.32 x 0.28 x 0.21
5.832 to 58.802	2.95 to 25.00	3.87 to 73.53
71723	44666	33755
11441 [0.0391]	8574 [0.0313]	9350 [0.0474]
11441/0/587	8574/0/605	9350/3/579
1.115	1.046	1.038
R_1 = 0.0224, wR_2 = 0.0460	R_1 = 0.0163, wR_2 = 0.0361	R_1 = 0.0549, wR_2 = 0.1471
1.08 and -1.22	0.534 and -0.499	3.436 and -3.035

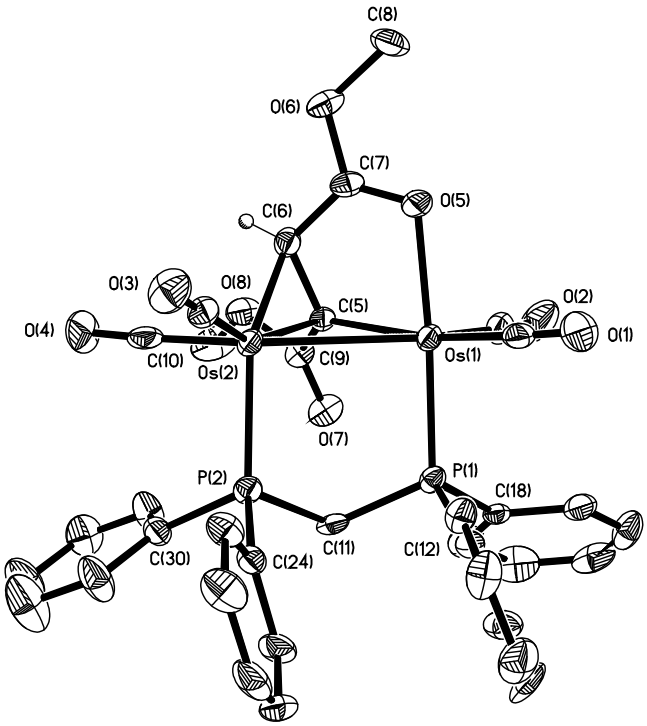

Fig. 1. ORTEP drawing of the molecular structure of $Os_2(CO)_4(\mu\text{-dppm})(\mu\text{-}\eta^2;\eta^1;\kappa^1\text{-}MeO_2CCCHCO_2Me)(\mu\text{-H})$ (**3a**) showing 50% probability thermal ellipsoids. Selected bond lengths (Å) and angles (^{o}): Os(1)-Os(2) 2.9254(6), Os(1)–P(1) 2.303(2), Os(2)–P(2) 2.346(2), Os(1)–C(5) 2.143(8), Os(1)–O(5) 2.170(6), Os(2)–C(5) 2.141(8), Os(2)–C(6) 2.177(9), C(5)–C(6) 1.460(11), C(6)–C(7) 1.437(12), C(5)–C(9) 1.455(12), O(5)–C(7) 1.237(10), Os(2)–C(5)–Os(1) 86.1(3), C(5)–Os(2)–C(6) 39.5(3), O(5)–Os(1)–P(1) 175.98(17), O(5)–Os(1)–Os(2) 85.42(16), P(1)–Os(1)–Os(2) 90.58(6), P(2)–Os(2)–Os(1) 92.55(6), P(1)–C(11)–P(2) 113.4(5), C(5)–C(6)–Os(2) 68.9(5), C(7)–O(5)–Os(1) 109.6(6).

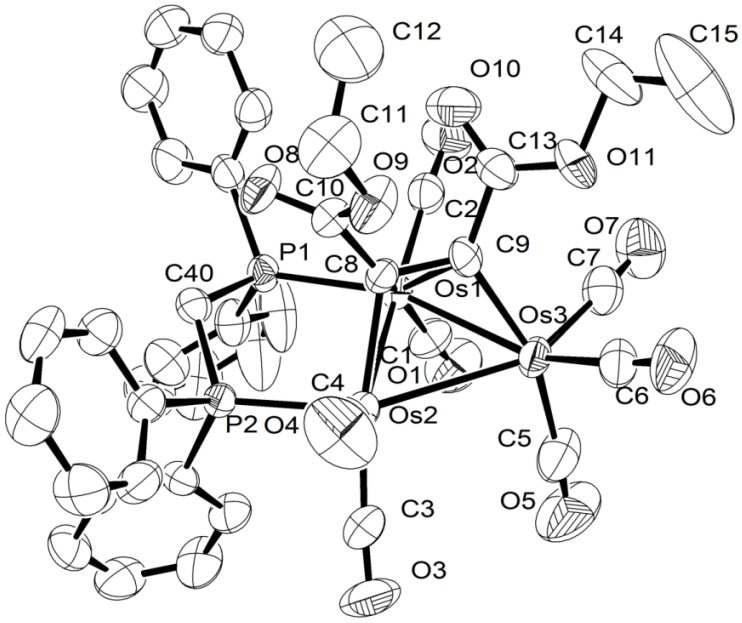

Fig. 2. ORTEP drawing of molecular structure of $Os_3(CO)_7(\mu\text{-dppm})(\mu_3\text{-}\eta^2;\eta^1;\eta^1\text{-}EtO_2CCCCO_2Et)(\mu\text{-}H)_2$ (**4b**) showing 50% probability thermal ellipsoids. Selected bond lengths (Å) and angles (°): Os(1)-Os(3) 2.7881(17), Os(1)-Os(2) 2.8729(19), Os(2)-Os(3) 3.0128(13), Os(1)-P(1) 2.355(3), Os(2)-P(2) 2.340(2), Os(1)-C(8) 2.251(8) Os(1)-C(9) 2.260(7), Os(2)-C(8) 2.153(8), Os(3)-C(9) 2.063(8), C(8)-C(9) 1.408(10), C(8)-C(10) 1.478(11), C(9)-C(13) 1.493(11); Os(1)-Os(2)-Os(3) 56.49(4), Os(1)-Os(3)-Os(2) 59.22(4), Os(3)-Os(1)-Os(2) 64.288(14), C(8)-Os(1)-C(9) 36.4(3), C(8)-Os(1)-Os(3) 70.70(19), C(8)-Os(1)-Os(2) 47.82(19), C(9)-Os(1)-Os(2) 68.8(2), C(9)-Os(1)-Os(3) 46.8(2), Os(3)-C(9)-Os(1) 80.2(3).

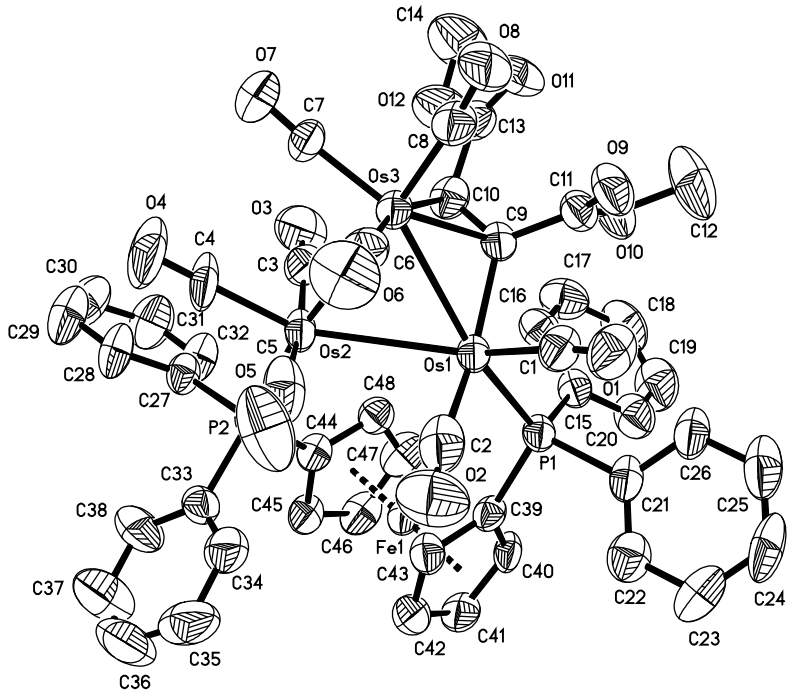

Fig. 3. ORTEP drawing of molecular structure of $Os_3(CO)_8(\mu\text{-dppf})(\mu_2\text{-}\eta^2;\eta^1;\eta^1\text{-}CH_3O_2CCHCCO_2CH_3)(\mu\text{-H})$ (**5a**) showing 50% probability thermal ellipsoids. Selected bond lengths (Å) and angles (°): Os(1)-Os(3) 2.8156(5), Os(1)-Os(2) 3.1191(5), Os(2)-Os(3) 2.9195(5), Os(1)-C(9) 2.097(9), Os(3)-C(9) 2.212(8), Os(3)-C(10) 2.274(9), Os(1)-P(1) 2.338(2), Os(2)-P(2) 2.377(2), C(9)-C(10) 1.435(13), C(9)-C(11) 1.495(13), C(10)-C(13) 1.509(14); Os(3)-Os(1)-Os(2) 58.670(13), Os(1)-Os(3)-Os(2) 65.865(14), Os(3)-Os(2)-Os(1) 55.464(12), C(9)-Os(3)-C(10) 37.3(3), P(1)-Os(1)-Os(2) 114.06(6), P(2)-Os(2)-Os(1) 117.57(6), C(9)-Os(1)-Os(2) 90.4(2), C(9)-Os(1)-Os(3) 51.0(2), C(9)-Os(3)-Os(1) 47.4(2), C(10)-Os(3)-Os(1) 75.8(2), C(10)-Os(3)-Os(2) 86.0(2), Os(1)-C(9)-Os(3) 81.6(3).

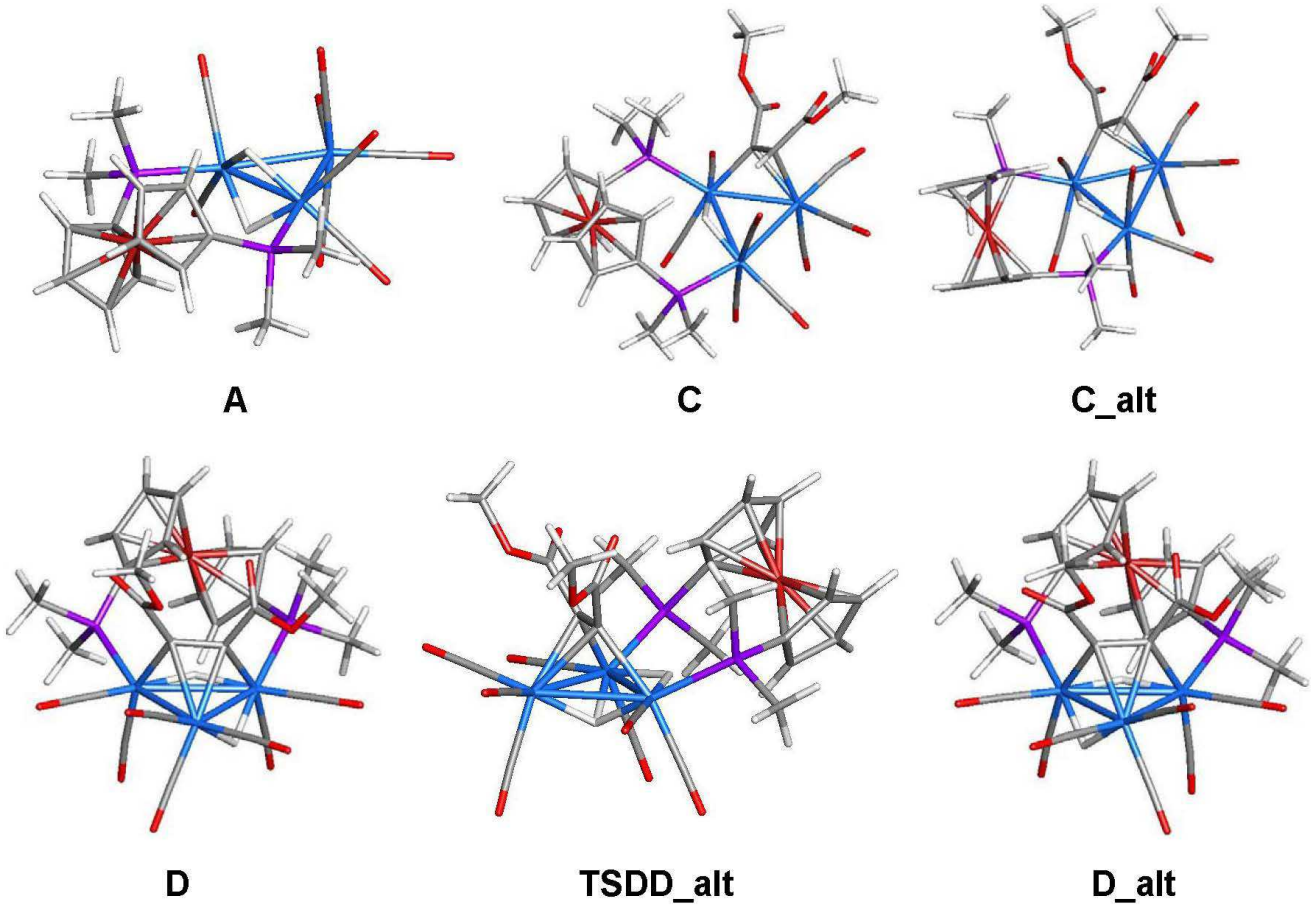

Fig. 4. B3LYP-optimized structures for cluster compounds **A**-**D_alt** and the transition state **TSDD_alt**. The structures for the alkyne DMAD (**B**) and liberated CO are not shown.

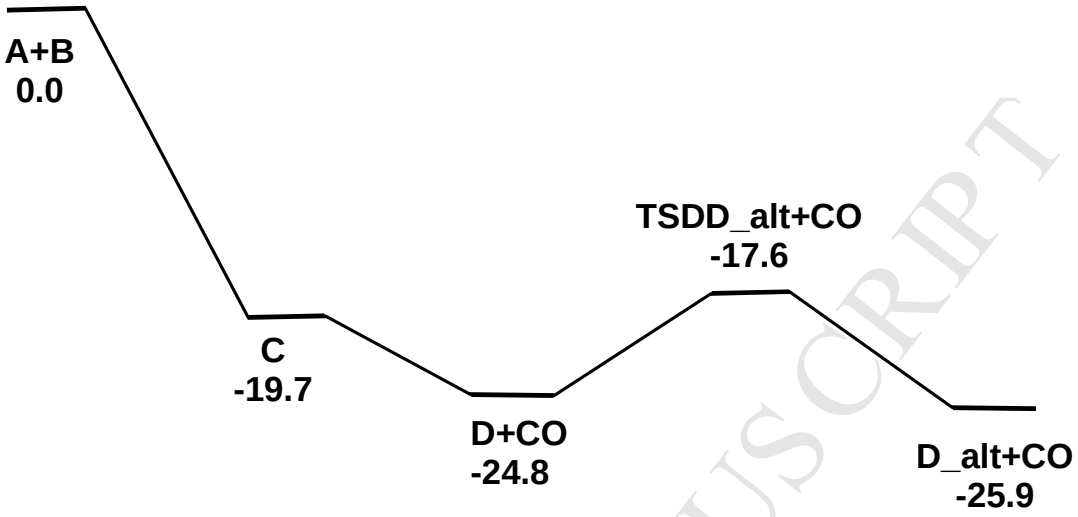

Fig. 5. Potential energy surface for the conversion of **A** and **B** to give **D_alt** and CO. Energy values are ΔG in kcal/mol with respect to **A** and **B**.

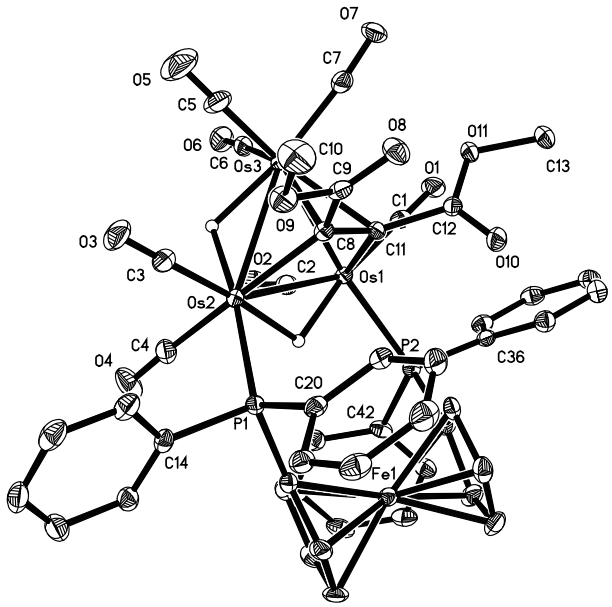

Fig. 6. ORTEP drawing of molecular structure of $Os_3(CO)_7(\mu\text{-dppf})(\mu_2\text{-}\eta^2;\eta^1;\eta^1\text{-}CH_3O_2CCC\text{-}CO_2CH_3)(\mu\text{-}H)_2$ (**6a**) showing 50% probability thermal ellipsoids. Selected bond lengths (Å) and angles (°): Os(1)-Os(2) 3.07188(17), Os(1)-Os(3) 2.79180(17), Os(2)-Os(3) 2.87256(17), Os(1)-P(2) 2.3437(8), Os(2)-P(1) 2.3588(8), Os(1)-C(11) 2.080(3), Os(3)-C(11) 2.300(3), Os(3)-C(8) 2.215(3), C(8)-C(11) 1.421(4), Os(2)-C(8) 2.129(3);Os(1)-Os(3)-Os(2) 65.665(4), Os(3)-Os(1)-Os(2) 58.433(4), Os(3)-Os(2)-Os(1) 55.902(4), Os(2)-C(8)-Os(3) 82.77(10), P(2)-Os(1)-Os(2) 115.944(19), P(1)-Os(2)-Os(1) 114.702(19), C(8)-Os(3)-C(11) 36.62(11), Os(1)-C(11)-Os(3) 79.03(10), C(8)-C(11)-Os(1) 114.9(2), C(8)-C(11)-Os(3) 68.44(16).

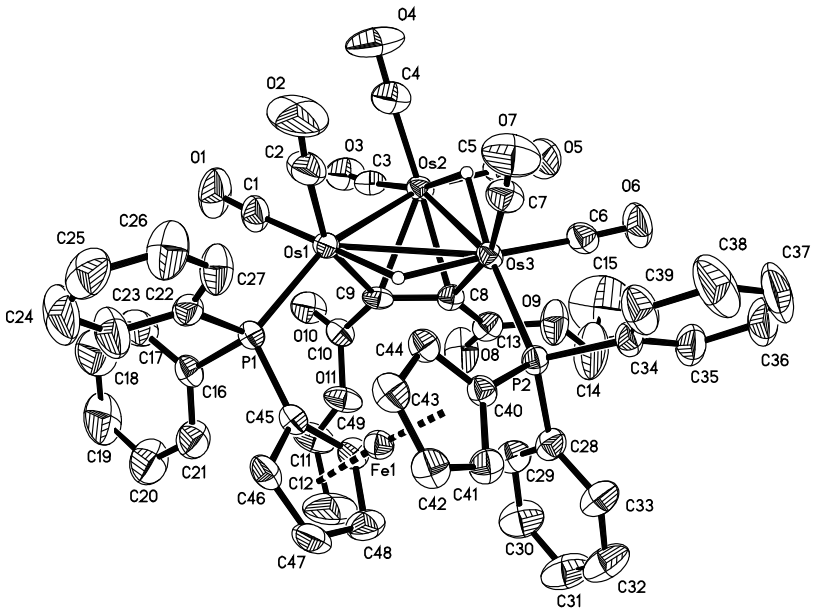

Fig. 7. ORTEP drawing of the molecular structure of $Os_3(CO)_7(\mu\text{-dppf})(\mu_3\text{-}\eta^2;\eta^1;\eta^1\text{-}EtOOCCCCOOEt)(\mu\text{-}H)_2$ (**6b**) showing 50% probability thermal ellipsoids. Selected bond lengths (Å) and angles (^{o}): Os(1)-Os(2) 2.7849(6), Os(1)-Os(3) 3.0685(6), Os(2)-Os(3) 2.8649(5), Os(1)-P(1) 2.3498(10), Os(3)-P(2) 2.3653(8), Os(1)-C(9) 2.084(3), Os(2)-C(8) 2.235(3), Os(2)-C(9) 2.308(3), Os(3)-C(8) 2.146(3), C(8)-C(9) 1.417(4), Os(1)-Os(2)-Os(3) 65.774(16), Os(2)-Os(1)-Os(3) 58.368(8), Os(2)-Os(3)-Os(1) 55.858(13), P(1)-Os(1)-Os(3) 117.71(2), C(8)-Os(2)-C(9) 36.29(11), C(9)-Os(2)-Os(1) 47.16(7), C(8)-Os(2)-Os(3) 47.82(8), P(2)-Os(3)-Os(1) 115.63(3), Os(3)-C(8)-Os(2) 81.66(10), Os(1)-C(9)-Os(2) 78.53(9).

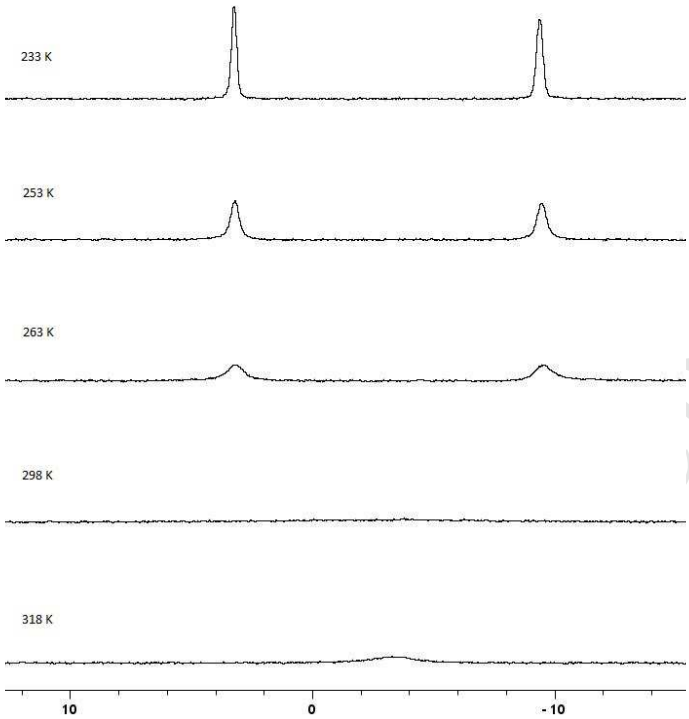

Fig. 8. VT $^{31}P\{^{1}H\}$ NMR spectra of **6a** recorded over the temperature range 298-233 K.

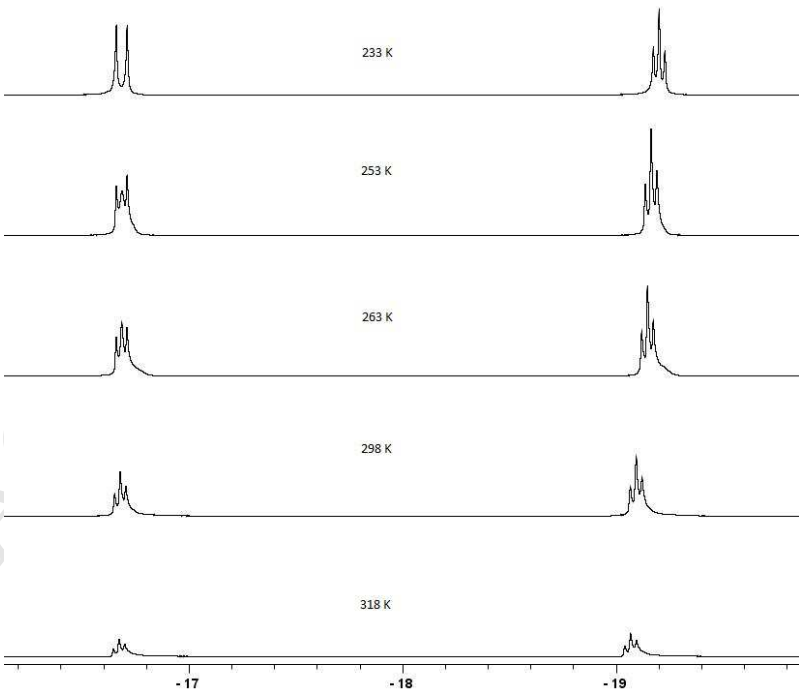

Fig. 9. VT ^{1}H NMR spectra of **6a** recorded over the temperature range 298-233 K.

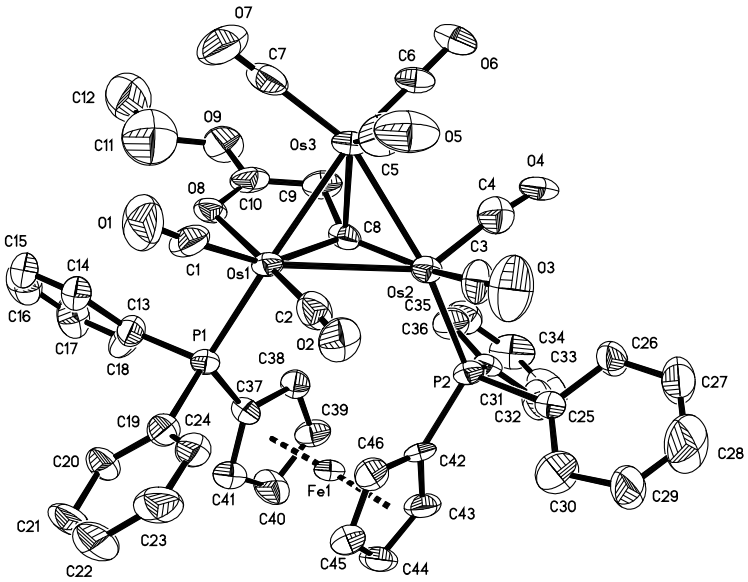

Fig. 10. ORTEP drawing of the molecular structure of $Os_3(CO)_7(\mu\text{-dppf})(\mu_3\text{-}\eta^{2;}\eta^1;\eta^1;\kappa^1\text{-}CCHCOOEt)]$ (**7b**) showing 50% probability thermal ellipsoids. Selected bond lengths (Å) and angles (°):Os(1)-Os(3) 2.7740(11), Os(1)-Os(2) 3.0481(11), Os(2)-Os(3) 2.8082(11), Os(1)-P(1) 2.390(5), Os(2)-P(2) 2.339(4),Os(1)-C(8) 2.138(15), Os(2)-C(8) 1.98(2), Os(3)-C(8) 2.185(17), Os(3)-C(9) 2.341(19),C(8)-C(9) 1.42(2), Os(1)-O(8) 2.134(12),Os(3)-Os(1)-Os(2) 57.45(3), Os(3)-Os(2)-Os(1) 56.37(3), Os(1)-Os(3)-Os(2) 66.19(3), Os(1)-C(8)-Os(3) 79.8(6), Os(2)-C(8)-Os(1) 95.4(8), Os(2)-C(8)-Os(3) 84.6(7), C(8)-Os(3)-C(9) 36.4(7), O(8)-Os(1)-Os(3) 82.2(2), O(8)-Os(1)-Os(2) 117.6(2), P(1)-Os(1)-Os(2) 116.00(11), P(2)-Os(2)-Os(1) 116.12(11).

Highlights

- New triosmium clusters containing bridging dppm/dppf and alkyne ligands
- Alkyne activation at diphosphine-bridged triosmium clusters
- Computational analysis of ligand fluxionality in triosmium clusters bearing flexible diphosphine and alkyne
- Reversible C-H bond activation at a triosmium centre
- Alkenyl to alkyne and hydride